

## Sterol 14 $\beta$ -Demethylase Structure-Based Design of VNI ((R)-N-(1-(2,4-dichlorophenyl)-2-(1H-imidazol-1-yl)ethyl)-4-(5-phenyl-1,3,4-oxadiazol-2-yl)benzamide) Derivatives to Target Fungal Infections: Synthesis, Biological Evaluation, and Crystallographic Analysis

Laura Friggeri, Tatiana Y Hargrove, Zdzislaw Wawrzak, Anna L. Blobaum, Girish Rachakonda, Craig W Lindsley, Fernando Villalta, W. David Nes, Maurizio Botta, F. Peter Guengerich, and Galina I Lepesheva

*J. Med. Chem.*, **Just Accepted Manuscript** • DOI: 10.1021/acs.jmedchem.8b00641 • Publication Date (Web): 12 Jun 2018

Downloaded from <http://pubs.acs.org> on June 12, 2018

### Just Accepted

“Just Accepted” manuscripts have been peer-reviewed and accepted for publication. They are posted online prior to technical editing, formatting for publication and author proofing. The American Chemical Society provides “Just Accepted” as a service to the research community to expedite the dissemination of scientific material as soon as possible after acceptance. “Just Accepted” manuscripts appear in full in PDF format accompanied by an HTML abstract. “Just Accepted” manuscripts have been fully peer reviewed, but should not be considered the official version of record. They are citable by the Digital Object Identifier (DOI®). “Just Accepted” is an optional service offered to authors. Therefore, the “Just Accepted” Web site may not include all articles that will be published in the journal. After a manuscript is technically edited and formatted, it will be removed from the “Just Accepted” Web site and published as an ASAP article. Note that technical editing may introduce minor changes to the manuscript text and/or graphics which could affect content, and all legal disclaimers and ethical guidelines that apply to the journal pertain. ACS cannot be held responsible for errors or consequences arising from the use of information contained in these “Just Accepted” manuscripts.



1  
2  
3  
4  
5 **Sterol 14 $\alpha$ -Demethylase Structure-Based Design of VNI ((*R*)-*N*-(1-(2,4-dichlorophenyl)-2-(1*H*-**  
6 **imidazol-1-yl)ethyl)-4-(5-phenyl-1,3,4-oxadiazol-2-yl)benzamide)) Derivatives to Target Fungal**  
7  
8  
9 **Infections: Synthesis, Biological Evaluation, and Crystallographic Analysis**  
10  
11  
12  
13

14 Laura Friggeri,<sup>†</sup> Tatiana Y. Hargrove,<sup>†</sup> Zdzislaw Wawrzak,<sup>§</sup> Anna L. Blobaum,<sup>¥</sup> Girish Rachakonda,<sup>‡</sup> Craig W.  
15  
16 Lindsley,<sup>¥</sup> Fernando Villalta,<sup>‡</sup> W. David Nes,<sup>‡</sup> Maurizio Botta,<sup>#</sup> F. Peter Guengerich<sup>†</sup>, and Galina I.  
17  
18 Lepesheva<sup>\*†,‡</sup>  
19  
20  
21  
22

23 <sup>†</sup>*Department of Biochemistry, Vanderbilt University School of Medicine, Nashville, Tennessee 37232, USA*

24 <sup>§</sup>*Synchrotron Research Center, Life Science Collaborative Access Team, Northwestern University, Argonne,*  
25 *Illinois 60439, USA*  
26  
27

28 <sup>¥</sup>*Vanderbilt Center for Neuroscience Drug Discovery, Franklin, Tennessee 37067, USA*  
29  
30

31 <sup>‡</sup>*Department of Microbiology and Immunology, Meharry Medical College, Nashville, Tennessee 37208, USA*  
32

33 <sup>#</sup>*Department of Chemistry and Biochemistry, Texas Tech University, Lubbock, Texas 79409, USA*  
34

35 <sup>#</sup>*Department of Biotechnology, Chemistry and Pharmacy, University of Siena, 53100 Siena, Italy*  
36  
37

38 <sup>‡</sup>*Center for Structural Biology, Vanderbilt University, Nashville, Tennessee 37232, USA*  
39  
40  
41  
42  
43  
44  
45  
46  
47  
48  
49  
50  
51  
52  
53  
54  
55  
56  
57  
58  
59  
60

**Abstract**

Due to the increase in the number of immunocompromised patients, the incidence of invasive fungal infections is growing but the treatment efficiency remains unacceptably low. The most potent clinical systemic antifungals (azoles) are the derivatives of two scaffolds: ketoconazole and fluconazole. Being the safest antifungal drugs, they still have shortcomings, mainly because of pharmacokinetics and resistance. Here we report the successful use of the target fungal enzyme, sterol 14 $\alpha$ -demethylase (CYP51), for structure-based design of novel antifungal drug candidates by minor modifications of VNI [(*R*)-*N*-(1-(2,4-dichlorophenyl)-2-(1*H*-imidazol-1-yl)ethyl)-4-(5-phenyl-1,3,4-oxadiazol-2-yl)benzamide]], an inhibitor of protozoan CYP51 that cures Chagas disease. Synthesis of fungi-oriented VNI derivatives, analysis of their potencies to inhibit CYP51s from two major fungal pathogens (*Aspergillus fumigatus* and *Candida albicans*), microsomal stability, effects in fungal cells, and structural characterization of *A. fumigatus* CYP51 in complexes with the most potent compound are described, offering a new antifungal drug scaffold and outlining directions for its further optimization.

## Introduction

In the last two decades, the mortality and morbidity of invasive fungal infections (IFIs) has greatly increased, and it has been estimated that over 1.6 million infected people die each year. The lack of access to timely diagnosis, co-infections with other diseases (HIV/tuberculosis), use of immunosuppressive therapies (chemotherapy/transplants), some medical devices (central venous catheters), and growing resistance to commercial antifungal drugs significantly contribute to the higher incidence of IFIs. In addition, the socio-economic environment in different countries has a great impact on antifungal treatment (i.e., expensive drugs and commercial availability).<sup>1</sup> Of the different fungal species, *Candida* and *Aspergillus* genera are responsible for the vast majority of life-threatening IFIs. *Candida albicans* remains the most prevalent human pathogen, yet non-*albicans Candida* species represent a growing global emergency. Highly virulent strains less susceptible to antifungal medicines, e.g. *C. auris*, a multidrug-resistant deadly pathogen, are often present in healthcare facilities.<sup>2</sup> *Aspergillus* is a ubiquitous fungus, transmitted to humans by inhalation of conidia. Approximately 200,000 cases of invasive aspergillosis, mostly in immunocompromised patients, are caused each year by *Aspergillus fumigatus*, which is also the major species responsible for chronic pulmonary aspergillosis and asthma.<sup>3</sup>

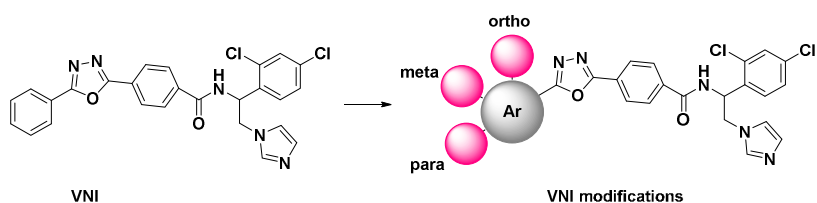
The therapeutic antifungal drugs available for systemic clinical use act on three different targets: 1) sterol biosynthesis (six azoles and terbinafine); 2) cell wall integrity (amphotericin B and caspofungin); and 3) DNA synthesis (flucytosine) (Supporting information, Figure S1A,C). All of these drugs have clinical limitations,<sup>4</sup> and therefore even upon treatment the mortality rates from IFIs often exceed 50%.<sup>3, 5</sup> More efficient new medicines are needed.

Several attempts to discover new fungal drug targets have been undertaken, and a few compounds with different modes of action are in preclinical studies.<sup>6</sup> Whether they will progress into clinical trials remain uncertain. On the other hand, further development of antifungal azoles, inhibitors of fungal sterol 14 $\alpha$ -demethylase (CYP51, EC 1.14.13.70), represents a successful area for investigation because azoles, compared to other classes of current systemic antifungals, clearly display higher potency, better safety

1  
2  
3 profile, and broader spectrum of activity.<sup>6-7</sup> Indeed, in 2015 a new azole, the triazole-based isavuconazole,  
4 was approved for treatment of IFIs,<sup>8</sup> while another triazole (albaconazole) and a tetrazole (VT-1161) are in  
5 clinical trials (Supporting information, Figure S1B) [<https://clinicaltrials.gov>].  
6  
7

8  
9 Determination of the crystal structures of *A. fumigatus*<sup>9</sup> and *C. albicans*<sup>10</sup> CYP51 in complexes with  
10 azole drugs (voriconazole and posaconazole) and drug candidates (VNI, VT-1161, and VT-1598<sup>11</sup>) opened  
11 new opportunities for rational, structure-based design of more efficient compounds. The objective of this  
12 work was to use the knowledge that we acquired from our structure/function studies to modify our  
13 experimental inhibitor of protozoan CYP51, VNI,<sup>12-13</sup> in such a way that its inhibitory effect on fungal CYP51  
14 is enhanced. We selected VNI because it is active *in vivo* against Chagas disease and visceral leishmaniasis,  
15 non-toxic, non-mutagenic, with excellent cellular permeability, metabolic stability, and pharmacokinetics  
16 (including oral bioavailability and tissue distribution that are substantially more favorable than those of  
17 systemic clinical antifungal azoles<sup>7</sup>). Moreover, although VNI is a relatively weaker inhibitor of fungal CYP51  
18 than the protozoan orthologs, we found that it is more effective in killing *A. fumigatus* cells than  
19 voriconazole, a first line drug against aspergillosis, with the minimum inhibitory concentration (MIC) values  
20 being 0.5 vs. 0.7  $\mu\text{g/mL}$ , respectively, for VNI and voriconazole.<sup>9</sup> Very importantly, the VNI scaffold is easy  
21 to synthesize and modify.  
22  
23  
24  
25  
26  
27  
28  
29  
30  
31  
32  
33  
34  
35

36 The rationale for this study was based on the observation that fungal and protozoan CYP51 structures,  
37 though displaying high 3-dimensional similarity, differ noticeably in the features of substrate entry, which in  
38 the fungal CYP51 structures is open much wider (due to the phylum-specific differences between the  
39 protozoan and fungal amino acid sequences).<sup>10</sup> The hypothesis to test was whether antifungal potency of  
40 the VNI scaffold can be enhanced through the formation of additional contacts between the inhibitor  
41 molecule and the substrate entrance residues of the fungal CYP51 enzyme.  
42  
43  
44  
45  
46  
47  
48  
49



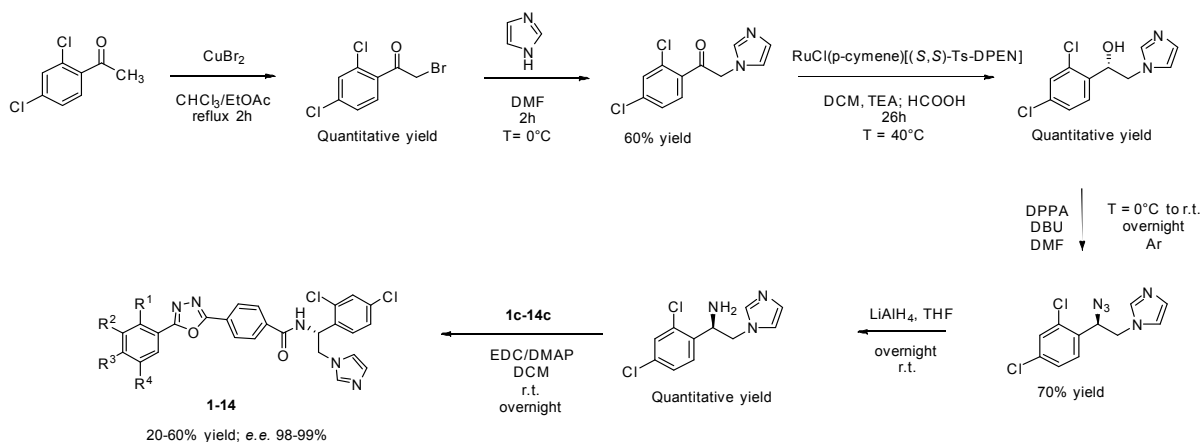
50  
51  
52  
53  
54  
55  
56  
57  
58  
59  
60  
**Figure 1. Sites of modifications in the VNI molecule**

A small in-house library of analogues carrying various substituents in the *ortho*, *meta*, and *para* positions of the distal (5-phenyl) ring of the VNI long arm (Figure 1) has been synthesized and analyzed, with the results serving as the initial proof of concept. Potencies of most of the new compounds to inhibit *C. albicans* and *A. fumigatus* CYP51 were increased, some of them approaching the potency of posaconazole, which is presently one of the most powerful inhibitors of fungal CYP51 (example shown in Table of Content Graphic).

## Results

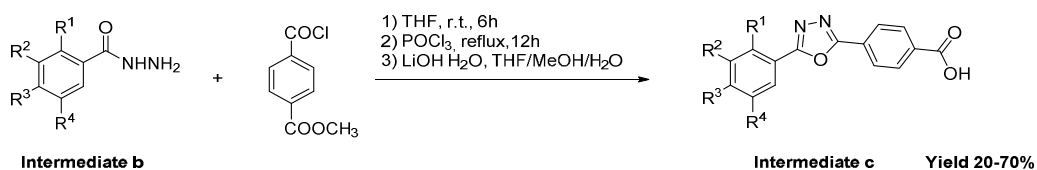
**Synthesis.** The new in-house library of VNI derivatives was prepared using the general procedures outlined in Scheme 1. The synthesis started by bromination of 1-(2,4-dichlorophenyl)-ethan-1-one, followed by condensation with the imidazole ring. Subsequently, asymmetric transfer hydrogenation with RuCl(p-cymene)[(S,S)-Ts-DPEN] catalyst was performed in order to obtain (S)-1-(2,4-dichlorophenyl)-2-(1H-imidazol-1-yl)ethan-1-ol, as described previously.<sup>14</sup> The direct conversion of (S)-1-(2,4-dichlorophenyl)-2-(1H-imidazol-1-yl)ethan-1-ol to (R)-1-(2-azido-2-(2,4-dichlorophenyl)ethyl)-1H-imidazole was carried out by dissolving the alcohol in *N,N*-dimethylformamide (DMF) and adding diphenyl phosphorazidate (DPPA) and 1,5-diazabicyclo[5.4.0]undec-7-ene (DBU) at 0 °C. (R)-1-(2,4-Dichlorophenyl)-2-(1H-imidazol-1-yl)ethan-1-amine was then prepared by reduction of the azide into an amine using LiAlH<sub>4</sub>.

### Scheme 1. Synthesis of new VNI derivatives.



The final compounds **1-14** were synthesized by coupling between (*R*)-1-(2,4-dichlorophenyl)-2-(1*H*-imidazol-1-yl)ethan-1-amine and 4-(5-phenyl-1,3,4-oxadiazol-2-yl)benzoic acids containing various substituents in the 5-phenyl ring (intermediate **c**, **Scheme 2**). The synthesis of intermediate **c** was performed using three reaction steps. The acylation of the hydrazide with methyl 4-(chlorocarbonyl)benzoate was followed by cyclization of the 1,3,4-oxadiazole in POCl<sub>3</sub>, and the hydrolysis of ester into carboxylic acid by LiOH·H<sub>2</sub>O.

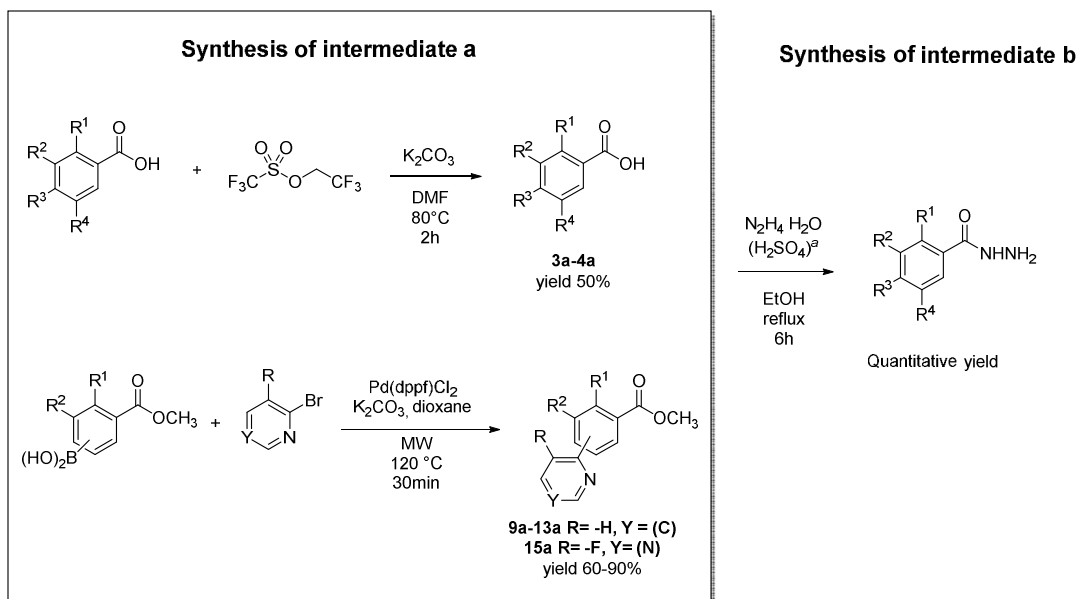
### Scheme 2. Synthesis of intermediate **c**.



- 1c:** R<sup>1</sup> = R<sup>4</sup> = -H; R<sup>2</sup> = R<sup>3</sup> = -F  
**2c:** R<sup>1</sup> = R<sup>4</sup> = -H; R<sup>2</sup> = -F; R<sup>3</sup> = -CF<sub>3</sub>  
**3c:** R<sup>1</sup> = -F; R<sup>2</sup> = R<sup>4</sup> = -H; R<sup>3</sup> = -OCH<sub>2</sub>CF<sub>3</sub>  
**4c:** R<sup>1</sup> = R<sup>3</sup> = -H; R<sup>2</sup> = -F; R<sup>4</sup> = -OCH<sub>2</sub>CF<sub>3</sub>  
**5c:** R<sup>1</sup> = R<sup>3</sup> = -H; R<sup>2</sup> = R<sup>4</sup> = -Cl  
**6c:** R<sup>1</sup> = R<sup>2</sup> = R<sup>3</sup> = -H; R<sup>4</sup> = -Br  
**7c:** R<sup>1</sup> = R<sup>2</sup> = R<sup>3</sup> = -H; R<sup>4</sup> = morpholinyl  
**8c:** R<sup>1</sup> = R<sup>2</sup> = R<sup>4</sup> = -H; R<sup>3</sup> = morpholinyl  
**9c:** R<sup>1</sup> = R<sup>2</sup> = R<sup>3</sup> = -H; R<sup>4</sup> = 2-pyridinyl  
**10c:** R<sup>1</sup> = R<sup>2</sup> = R<sup>4</sup> = -H; R<sup>3</sup> = 2-pyridinyl  
**11c:** R<sup>1</sup> = R<sup>3</sup> = -H; R<sup>2</sup> = -F; R<sup>4</sup> = 2-pyridinyl  
**12c:** R<sup>1</sup> = -F; R<sup>2</sup> = R<sup>4</sup> = -H; R<sup>3</sup> = 2-pyridinyl  
**13c:** R<sup>1</sup> = -F; R<sup>2</sup> = R<sup>3</sup> = -H; R<sup>4</sup> = 2-pyridinyl  
**14c:** R<sup>1</sup> = R<sup>4</sup> = -H; R<sup>2</sup> = -Cl; R<sup>3</sup> = -SO<sub>2</sub>CH<sub>3</sub>  
**15c:** R<sup>1</sup> = R<sup>3</sup> = -H; R<sup>2</sup> = -F; R<sup>4</sup> = 5-fluoro-6-pyrimidinyl

However, different approaches were used for preparing variously substituted benzohydrazines (intermediate **b**). Thus, **1b** and **6b** were available commercially, the intermediates **b** for compounds **2**, **5**, **7**, **8**, and **14** were synthesized by the addition of the hydrazine monohydrate (N<sub>2</sub>H<sub>4</sub>·H<sub>2</sub>O) to the commercial available carboxylic acid or ester, as shown in Scheme 3. The synthesis of intermediates **b** for **3**, **4**, and **9-13** included preparation of intermediates **a**. Intermediates **a** for compounds **3** and **4** were made by addition of the electrophile 2,2,2-trifluoroethyl trifluoromethanesulfonate to the corresponding carboxylic acid. Intermediates **a** for **9-13** were synthesized using [1,1'-bis(diphenylphosphino)ferrocene]dichloropalladium(II) (Pd(dppf)Cl<sub>2</sub>) as a catalyst for Suzuki coupling, and it was performed in a microwave reactor to increase the efficiency (Scheme 3).

## Scheme 3. Synthesis of benzohydrazines.




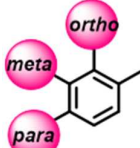
<sup>a</sup>  $\text{H}_2\text{SO}_4$  was not used for hydrazinolysis of **9a-13a**.

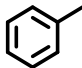
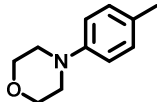
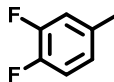
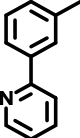
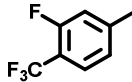
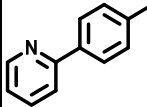
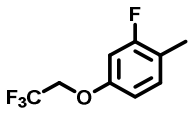
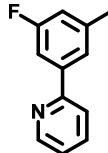
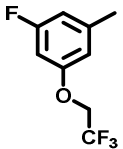
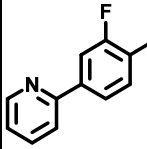
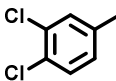
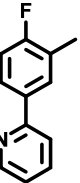
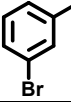
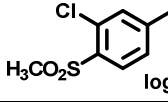
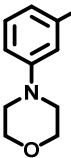
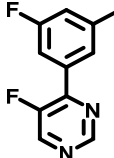
**Evaluation of new compounds as inhibitors of fungal CYP51 activity.** Even minor modifications in the 5-phenyl ring composition produced remarkably strong effects on the potencies of the new compounds to inhibit enzymatic activity of *C. albicans* and *A. fumigatus* CYP51 (Table 1). Thus, quite encouragingly, addition of only two fluorine atoms, in the *meta* and *para* positions relative to 1,3,4-oxadiazole (Figure 1) (compound **1**, 5-(3,4-difluorophenyl)-1,3,4-oxadiazole), enhanced inhibition of *C. albicans* CYP51 activity from 20 to 90% and inhibition of *A. fumigatus* CYP51 activity from 24 to 60% (under the same conditions the inhibitory effects of posaconazole were 98 and 93%, respectively). When chlorines were substituted for fluorines (atomic radius 0.99 Å vs. 0.71 Å) in the same *meta* and *para* positions (compound **5**), the inhibitory effect on *C. albicans* increased slightly (92%) but inhibition of *A. fumigatus* CYP51 became weaker (55%). Because the larger size of a chlorine atom did not appear to be crucial for inhibition, and introduction of a fluorine has a lower impact on drug lipophilicity (e.g., the logP values of **1** and **5** are 4.88 and 5.68, respectively, Table 1), we mainly used fluorine instead of chlorine substituents in other (non-



aromatic) analogues, except for compound **14** (logP 3.83), whose potency towards both fungal enzymes turned out to be about 2-fold lower than that of **5**. On the other hand, substitution of a *para* fluorine with a trifluoromethyl group in **2** (logP 5.65), increased the ability of the compound to inhibit *A. fumigatus* (68%) without influencing its inhibition of *C. albicans* CYP51 (89%). Our strongest inhibitor, compound **3**, has one fluorine atom in the *ortho* position and a trifluoroethoxy group in the *para* position (94% and 82% inhibition of *C. albicans* and *A. fumigatus* CYP51 activity, respectively). However, when the same substituents are in two *meta* positions, compound **4**, the potency drops, although the inhibitory effect is still more than twice that of the parent compound VNI. Since all of the modifications above produced inhibitors with higher potencies, thus supporting our hypothesis, a number of bulkier substituents were introduced to decorate the 5-phenyl ring of the VNI arm. A single bromine atom (atomic radius 1.14 Å) in the *meta* position (compound **6**) enhanced the inhibition to 84% (*C. albicans*) and to 41% (*A. fumigatus*). When the *meta* position was substituted with a morpholine ring however (compound **7**), the potency for inhibition of *A. fumigatus* CYP51 decreased (15% inhibition), and insertion of a morpholine ring into the *para* position produced an even weaker inhibitor (compound **8**, 29% and 3% inhibition towards *C. albicans* and *A. fumigatus* CYP51, respectively). While it is possible that the morpholine substitutions are unfavorable as a result of the ring hydrophilicity, because the CYP51 substrate entry, being immersed into the endoplasmic reticulum membrane *in vivo*, is composed mainly of hydrophobic amino acid residues, a general trend of the *meta* position being more preferable than the *para* position for a heterocyclic substituent is apparent (compounds **9**, **10**, **11**, **12**, **13**, and **15** in Table 1). Among these six analogues, **11** and **15** were most potent towards both fungal enzymes (87/80% and 92/57%, *C. albicans*/*A. fumigatus* CYP51, respectively).

**Table 1. New VNI analogues: 5-phenyl ring composition and inhibition of fungal CYP51 activity <sup>a</sup>.**

Cmp		CYP51 inhibition, %		Cmp		CYP51 inhibition, %	
		<i>C. albicans</i>	<i>A. fumigatus</i>			<i>C. albicans</i>	<i>A. fumigatus</i>

VNI	 logP 4.57	20 ± 3	24 ± 6	8	 logP 4.45	29 ± 3	3 ± 1
1	 logP 4.88	90 ± 3	58 ± 3	9	 logP 5.33	77 ± 3	34 ± 4
2	 logP 5.65	89 ± 2	65 ± 13	10	 logP 5.33	66 ± 6	23 ± 1
3	 logP 5.58	94 ± 1	82 ± 4	11	 logP 5.49	87 ± 3	80 ± 5
4	 logP 5.58	65 ± 4	51 ± 5	12	 logP 5.49	61 ± 4	26 ± 4
5	 logP 5.68	92 ± 3	55 ± 4	13	 logP 5.49	83 ± 1	24 ± 5
6	 logP 5.4	84 ± 4	41 ± 4	14	 logP 3.83	53 ± 1	32 ± 3
7	 logP 4.45	58 ± 2	15 ± 1	15	 logP 5.05	92 ± 1	57 ± 1

<sup>a</sup>A 1-hour reaction was used to distinguish the strongest inhibitors, with the potential propensity to act as functionally irreversible (see Experimental Section, Discussion). The P450 concentration was 0.5  $\mu\text{M}$  and the molar excess of each inhibitor over enzyme was 1.5-fold (0.75  $\mu\text{M}$ ).

**Evaluation of selected compounds as CYP51 binding ligands.** Five the strongest inhibitors of *C. albicans* and *A. fumigatus* CYP51 activity were also assayed as binding ligands of the enzymes (Table 2). VNI, posaconazole, and voriconazole were used as controls. Previously we observed a clear lack of correlation between the apparent spectral binding affinities of some ligands and their potencies to inhibit CYP51 enzymatic activity, particularly in long reactions.<sup>14-16</sup> Accordingly we compared spectral titrations with close

structural analogues (e.g., as observed in ref. 17). Overall, the data support a relationship between binding and inhibitory potency, particularly for compounds **1**, **2**, and **3**, which have the highest structural similarities to VNI (see Table 1 and Supplemental Fig S2).

**Table 2.** Dissociation constants determined by spectral titration of *C. albicans* and *A. fumigatus* CYP51 with VNI, compounds **1**, **2**, **3**, **11**, and **15**, posaconazole and voriconazole.

Cmpds	<i>C. albicans</i>	Fold enhancement	<i>A. fumigatus</i>	Fold enhancement
	$K_d$ , nM	$(K_d \text{ VNI}/K_d n^a)$	$K_d$ , nM	$(K_d \text{ VNI}/K_d n)$
VNI	290 ± 27	-	203 ± 10	-
<b>1</b>	13 ± 1	22	57 ± 6	4
<b>2</b>	13 ± 1	22	55 ± 3	4
<b>3</b>	10 ± 6	29	20 ± 4	10
<b>11</b>	25 ± 5	12	61 ± 3	3
<b>15</b>	95 ± 11	3	132 ± 2	1.5
Posaconazole	81 ± 16	3.5	131 ± 11	1.5
Voriconazole	165 ± 9	1.8	56 ± 4	3.6

<sup>a</sup>n – compound number

**Estimated intrinsic and hepatic clearance in human, rat, and mouse microsomes.** Since high metabolic stability is one of the many advantages of VNI as a potential drug,<sup>18</sup> we examined the parameters for the new compounds. Moreover, simultaneous analysis in human and animal microsomes is highly informative in allowing for a prediction of the likelihood of acceptable pharmacokinetics in clinical trials. VNI and thirteen new compounds with the increased potencies to inhibit both fungal CYP51 enzymes (all except for the morpholine-containing **7** and **8**) were tested in human, rat, and mouse liver microsomes (Table 3). The data show that overall, none of the modifications drastically affected the stability of the new compounds, with all but one (**11**, human microsomes) displaying low to moderate hepatic clearance. The stability of

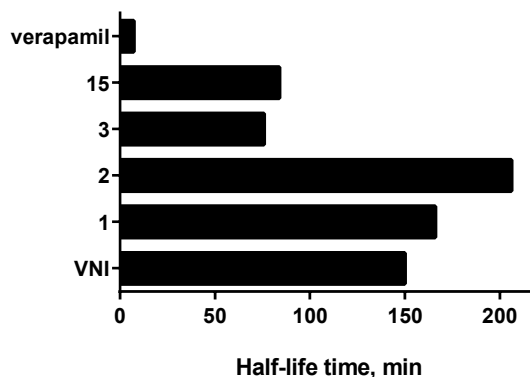
compounds **1** and **2** in human and mouse systems was even higher than that of VNI. Replacement of the two fluorine atoms with chlorine (**5**), however, had slightly negative effects in human/mouse but not in rat microsomes. Although the pyridine ring can be metabolically vulnerable,<sup>19</sup> compounds **9** and **12-13** also showed rather good stability, not inferior to compound **15** (5-fluoro-6 pyrimidinyl analogue of **11**).

**Table 3. Microsomal stability: Half-lives and estimated clearance of VNI and new derivatives in human, rat, and mouse microsomes.**

Cmpds	Human			Rat			Mouse		
	CL <sub>INT</sub> <sup>a</sup>	CL <sub>HEP</sub>	t <sub>½</sub> (min) <sup>b</sup>	CL <sub>INT</sub>	CL <sub>HEP</sub>	t <sub>½</sub> (min)	CL <sub>INT</sub>	CL <sub>HEP</sub>	t <sub>½</sub> (min)
VNI	8.31	5.95	150	26.4	19.2	106	87	44	62
<b>1</b>	7.53	5.54	166	31	21	91	55	34	98
<b>2</b>	6.06	4.07	206	36	24	77	60	36	92
<b>3</b>	16.5	9.24	76	64	34	44	88	44	62
<b>4</b>	11.3	7.33	111	50.4	29	56	84.7	43.6	65
<b>5</b>	11.4	7.39	110	70	35	40	107	49	51
<b>6</b>	9.47	6.53	132	27	19	106	126	55	43
<b>9</b>	13.1	8.06	95	68	35	41	152	56	36
<b>10</b>	10.8	7.15	115	94	40	30	95	46	57
<b>11</b>	96.6	17.3	13	36.0	24.0	78	55.0	34	99
<b>12</b>	15	8.75	83	51.6	29.7	54	36.5	26.0	149
<b>13</b>	10.2	6.85	123	49.4	29.0	57	238	65	23
<b>14</b>	9.31	6.45	134	104	42	27	56	34.5	97

<b>15</b>	14.9	8.37	84	27.0	19.5	104	104	48.3	52
-----------	------	------	----	------	------	-----	-----	------	----

<sup>a</sup> Intrinsic ( $CL_{INT}$ ) and hepatic clearance ( $CL_{HEP}$ ) expressed in mL/min/kg body weight; <sup>b</sup> *in vitro* half-life values in minutes.



**Figure 2.** Half-life time of VNI, selected analogues, and a drug verapamil (positive control) in human microsomes.  $R^2$  values were all  $>0.7$ .

**Cellular effects in *A. fumigatus* strains.** Four compounds (**1**, **2**, **3**, and **15**) that revealed both the highest potencies to inhibit *A. fumigatus* CYP51 activity and favorable stability in human microsomes (Figure 2) were further tested in cellular experiments. VNI was used as a control (Table 4). All the derivatives displayed stronger inhibition of fungal cell growth, and their fungicidal potencies correlated well with the effects on the target enzyme. The lowest MIC values, 2.4- and 2.5-fold lower than the MICs of VNI on average, were observed for compounds **2** and **3**, respectively.

**Table 4.** Antifungal activity of VNI and derivatives (MIC  $\pm$ SEM,  $\mu$ g/mL)

<i>A. fumigatus</i> strain	VNI	<b>1</b>	p-value	<b>2</b>	p-value	<b>3</b>	p-value	<b>15</b>	p-value
1022	0.48 + 0.05	0.29(+0.03)	0.0001*	0.19(+0.03)	0.0003*	0.19(+0.03)	0.0002*	0.48(+0.05)	1
32820	0.08 + 0.03	0.08(+0.03)	0.0009*	0.09(+0.02)	0.0027*	0.06(+0.01)	0.0004*	0.19(+0.03)	0.21
MYA-3626	0.08 + 0.03	0.78(+0.03)	0.0035*	0.39(+0.05)	0.0001*	0.39(+0.05)	0.0001*	0.78(+0.04)	0.0035*

\*Statistical significance of the differences (p values) was analyzed by one-way ANOVA

1  
2  
3 **X-ray crystallography.** The compound (**3**) that displayed the strongest inhibition of both fungal CYP51  
4 enzymes (Table 1) and the most expressed enhancement in the apparent binding affinity (29 and 10-fold in  
5 comparison to VNI, *C. albicans* and *A. fumigatus* CYP51, respectively, Table 2) was selected for co-  
6 crystallization. In addition to the goal of observing inhibitor-specific interactions with the enzyme (i.e.,  
7 structural basis for the increased inhibitory potency), we examined whether the modifications alter the  
8 ligand orientation in the fungal CYP51 substrate binding cavity. While the co-crystals of *C. albicans* CYP51  
9 with **3** did not diffract well, the *A. fumigatus* complexes produced crystals that diffracted to ~2.4 Å. Several  
10 datasets were collected, the structures were determined, and each of them indicated that upon binding to  
11 the enzyme the inhibitor can adopt two different conformations, both of them different from the  
12 conformations of VNI in *A. fumigatus* or in *T. brucei* CYP51 (Figure 3A). The structure of the best diffracting  
13 crystal has been refined and deposited in the Protein Data Bank (PDB 6CR2). Supplementary Table S4  
14 summarizes the diffraction and refinement statistics. The  $2F_o-F_c$  electron density maps of the inhibitor  
15 molecules in both conformations contoured at  $1.2 \sigma$  and are shown as gray mesh can be seen in the Table  
16 of Content Graphic.  
17  
18  
19  
20  
21  
22  
23  
24  
25  
26  
27  
28  
29  
30  
31  
32  
33

## 34 **Discussion and Conclusions**

35  
36  
37

38 It has been known for years that antifungal azoles, both clinical drugs and agricultural fungicides, kill  
39 fungal cells by inhibiting their sterol biosynthesis at the stage of  $14\alpha$ -demethylation of sterol precursors.<sup>20</sup>  
40 This is a three-step reaction catalyzed by a single cytochrome P450 monooxygenase, named sterol  $14\alpha$ -  
41 demethylase<sup>21</sup> (CYP51). This target enzyme, being a highly hydrophobic membrane-bound protein, has  
42 never actually been directly utilized in the process of drug discovery or development.<sup>7</sup>  
43  
44  
45  
46  
47

48 In part because of this, the process of antifungal drug discovery has been slow, costly, and low-efficient.<sup>6</sup>  
49 The six clinical systemic azoles, which represent the major portion of the current arsenal of clinical  
50 antifungal drugs, are derivatives of two inhibitory scaffolds: ketoconazole (itraconazole and posaconazole)  
51 and fluconazole (voriconazole and isavuconazole) (Supplementary Figure S1A). The third, a tetrazole-based  
52 scaffold from Viamet (Supplementary Figure S1B), is currently in trials. All these drugs were discovered  
53  
54  
55  
56  
57  
58  
59  
60

1  
2  
3 rather empirically by monitoring effects of hundreds of compounds on fungal cell growth. Our study shows  
4 that direct analysis of CYP51 enzyme inhibition can be utilized to shift the traditional drug discovery  
5 paradigm, making it potentially much more effective.  
6  
7

8  
9 All of the 15 compounds synthesized and analyzed in this work, including the parent compound VNI,<sup>9</sup>  
10 inhibit the initial rate of fungal CYP51 reactions when added at an equimolar ratio to the enzyme, thus  
11 producing IC<sub>50</sub> values of ~0.25 μM, corresponding to one-half of the enzyme concentration in the reaction  
12 mixture (data not shown). However, as seen in Table 1, with time some of the inhibitors are replaced by the  
13 substrate in the fungal CYP51 active site more easily than the others, although most of the (5-phenyl) ring  
14 substituents (presumably positioned in close proximity to the CYP51 substrate entry) increase potencies of  
15 the inhibitors to hold the enzyme in the catalytically inactive state.  
16  
17  
18  
19  
20  
21  
22

23  
24 Azoles are generally known as competitive reversible heme coordinating inhibitors of cytochromes  
25 P450.<sup>22</sup> However, as it was first observed in 1987 for CYP51 from *S. cerevisiae*<sup>23</sup> and later rediscovered by  
26 our research group for protozoan CYP51,<sup>16</sup> some azole-based inhibitors can act in a functionally irreversible  
27 manner due to their high affinity. Added at a concentration equimolar to the enzyme, they entirely inhibit  
28 CYP51 catalysis and cannot be replaced by the substrate for an extended period of time, even though no  
29 covalent bonds with the protein are formed.<sup>7</sup> VNI is an example of such an inhibitor for trypanosomal  
30 CYP51, while VT-1161, VF-1598, and posaconazole can serve as examples of such inhibitors for fungal  
31 CYP51.  
32  
33  
34  
35  
36  
37  
38  
39

40  
41 The very strong affinity of some of the azoles appears to be somehow connected with the strict  
42 functional phylogenetic conservation of CYP51 and the three-step stereoselective oxidation reaction  
43 sequence, which together require high structural rigidity of the enzyme active site.<sup>24</sup> Indeed, none of more  
44 than 30 crystal structures of microbial CYP51s bound to various inhibitory chemotypes that we have  
45 determined have displayed any large-scale rearrangements in the active site backbone upon inhibitor  
46 binding. Fortunately for antifungal drug design, the active site of human CYP51 appears to be much more  
47 flexible,<sup>25-27</sup> rendering the human enzyme naturally resistant to inhibition, at least with all ever tested  
48  
49  
50  
51  
52  
53  
54  
55  
56  
57  
58  
59  
60

1  
2 antimicrobial azoles, both commercial and experimental,<sup>26</sup> a favorable feature that enables pathogen-  
3 selectivity of CYP51-targeting antimicrobial agents.  
4  
5

6  
7 In the protozoan CYP51 structures, VNI<sup>12</sup> and its derivatives VFV and VNT<sup>18</sup> all form hydrogen bonds  
8 with the amino acid residues in the central, catalytic area of the CYP51 active site. The VT tetrazoles form  
9 H-bonds with the fungal-specific histidine (His-374 in *A. fumigatus* and His-377 in *C. albicans*) that lines the  
10 CYP51 substrate access channel.<sup>10-11</sup> CYP51 complexes with posaconazole do not involve any H-bond  
11 formation but display multiple enzyme-inhibitor contacts around the substrate entry.<sup>10</sup>  
12  
13  
14  
15

16  
17 Binding of VNI to *A. fumigatus* CYP51 does not produce any H-bonds, and its three ring arm is not long  
18 enough to reach the substrate entry site. Nevertheless, in addition to the strong (2.0 Å) coordination bond  
19 between its imidazole (N3) nitrogen and the enzyme heme iron, VNI forms van der Waals contacts with 19  
20 amino acid residues, including the sandwich  $\pi$ - $\pi$  stacking interactions with Phe-234.<sup>9</sup> This bonding provides  
21 a structural background for the strong inhibitory effect of VNI on the initial fungal CYP51 reaction and the  
22 reversibility of inhibition in the presence of the substrate. The results support our hypothesis that  
23 elongation of the VNI arm is likely to increase its potency as fungal CYP51 inhibitor.  
24  
25  
26  
27  
28  
29  
30  
31

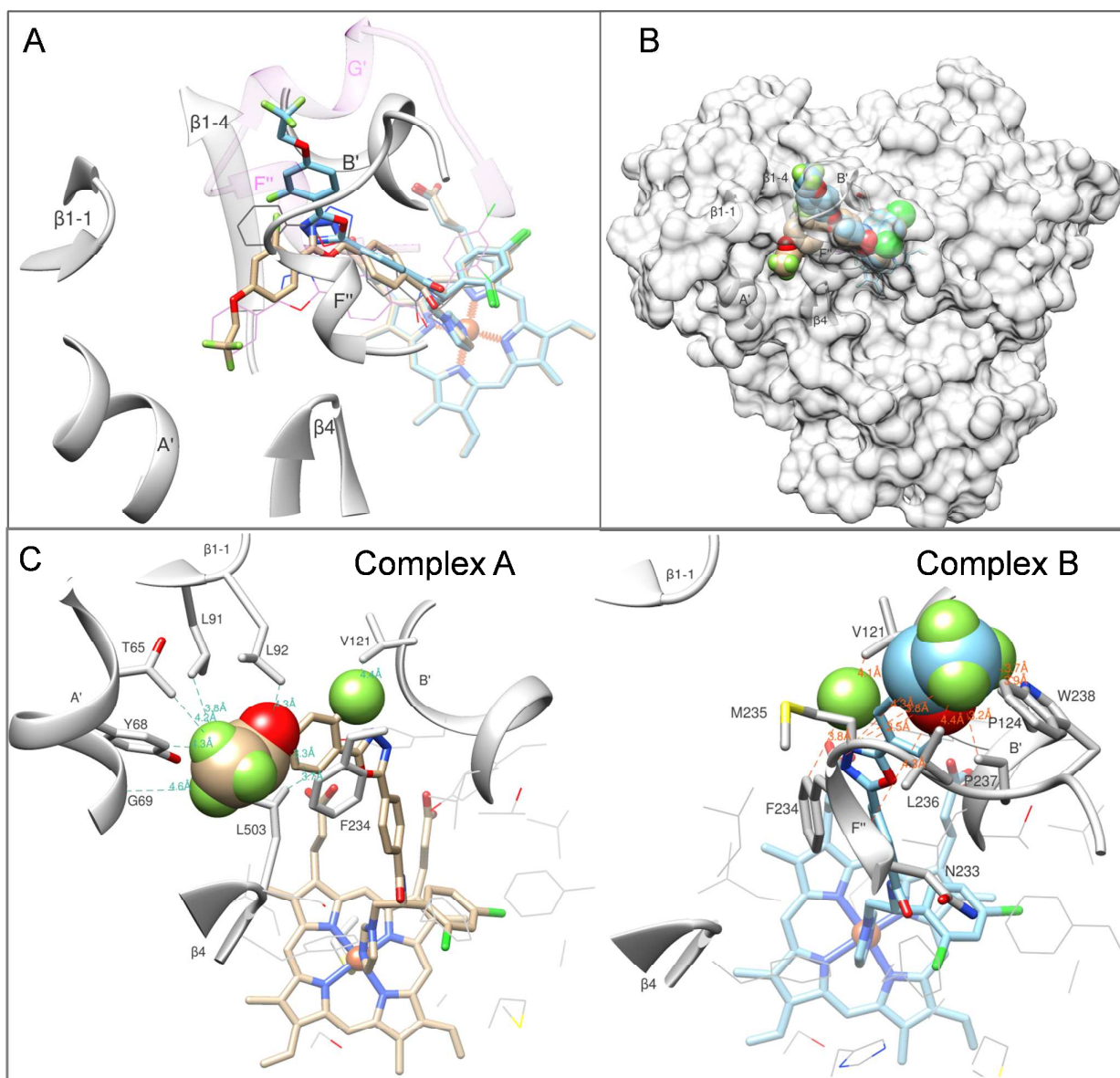
32 The crystal structure of *A. fumigatus* CYP51 complexed with compound **3** (ligand PDB ID Lfv) shows that  
33 the stronger enzyme inhibition is indeed due to the new interactions around the substrate entry (Figure 3B)  
34 and also suggests that larger substituents here might be even more efficient. In both conformations Lfv  
35 forms contacts with an additional seven amino acid residues of the enzyme (Figure 3C). In molecule A  
36 (CYP51-common portion of the substrate entry), Thr-65, Tyr-68, Gly-69 (helix A'), Leu-91, Leu-92 ( $\beta$ 1  
37 hairpin), and Phe-234 (helix F') interact with the trifluoroethoxy moiety, and Val-121 (helix B') interacts  
38 with the fluorine atom inserted into the *ortho* position relative to the oxadiazole ring. In molecule B (fungal  
39 CYP51-specific portion of the substrate entry), Asn-233, Phe-234, Met-235, Leu-236, Pro-237, and Trp-238  
40 (helix F') interact with the trifluoroethoxy moiety, while Val-121 and Phe-124 (helix B') interact with the  
41 additional *ortho* fluorine. Interestingly, in both complexes Phe-234 "follows" the inhibitor orientation,  
42 preserving the  $\pi$ - $\pi$  stacking interactions with its 5-phenyl aromatic ring (see also Table of Content Graphic,  
43 right panel). It remains to be clarified if one of the two Lfv conformations warrants a higher inhibitory  
44  
45  
46  
47  
48  
49  
50  
51  
52  
53  
54  
55  
56  
57  
58  
59  
60



1  
2  
3 potency, but it appears that such a probability for complex B may be higher. In this complex, a fluorine  
4  
5 atom of the LFV trifluoroethoxy moiety displays a propensity to form H-bond like interactions with the main  
6  
7 chain oxygen of Met-235 (2.3 Å) and with the indole nitrogen of Trp-238 (3.2 Å), while the ethoxy oxygen is  
8  
9 positioned only 3.5 Å from the main chain oxygen of Phe-234 (Supplementary Figure S3). All these three  
10  
11 residues are in helix F'', the CYP51 area that is most likely to serve as part of the "lid" for the substrate  
12  
13 entry. Assuming that binding of the substrate requires opening of the FG-lid, these contacts with the ligand  
14  
15 are likely to restrict the required movement. No such gatekeeping interactions are seen in complex A.

16  
17 Further efforts directed towards strengthening fungal CYP51-VNI scaffold interactions are in progress,  
18  
19 with our ultimate goal being to design very high affinity compounds that will bind to the fungal CYP51 most  
20  
21 efficiently, keeping the enzyme in its catalytically inactive state and preventing a conformational switch  
22  
23 required for the interaction with the electron donor partner NADPH-cytochrome P450 reductase.

24  
25 Overall, the results of this study prove that structure-based design is useful for the target fungal CYP51,  
26  
27 meaning that novel potent inhibitory scaffolds can be rationally built. Minor modifications may be sufficient  
28  
29 to optimize pharmacokinetics and thus to improve the IFI treatment efficiency and retard drug resistance.  
30  
31 The availability of various alternative CYP51 inhibitory scaffolds should be extremely useful in overcoming  
32  
33 situations in which patients succumb to fungal sepsis simply because they must be temporarily  
34  
35 immunosuppressed and there are no efficient drugs available.  
36  
37  
38  
39  
40  
41  
42  
43  
44  
45  
46  
47  
48  
49  
50  
51  
52  
53  
54  
55  
56  
57  
58  
59  
60



**Figure 3.** LFV (compound 3) adopts two alternative conformations in the active site of *A. fumigatus* CYP51B. **A.** Substrate entry area. The carbon atoms in the superimposed structures of complexes A and B are tan and blue, respectively. The corresponding orientation of VNI in the structures of *A. fumigatus* CYP51B (PDB ID 4uy1, gray lines) and *Trypanosoma brucei* CYP51 (PDB ID 3gw9, purple lines) are shown for comparison. The *A. fumigatus* CYP51 substrate entry-defining secondary structural elements are presented as gray ribbon and labeled. The semitransparent ribbon of the (longer) F/G loop area in the protozoan CYP51 (3gw9) is purple, and the F' helix and the protozoan-specific G' helix are labeled. **B.** Overall view in semitransparent surface representation. **C.** New ligand/enzyme interactions formed as a result of the VNI modification. Atoms added to the VNI structure are presented as spheres. The amino acid residues of *A. fumigatus* CYP51B involved in the additional interactions are shown as stick models and labelled, and selected distances are displayed.

## Experimental Section

**Chemical Synthesis.** All reagents and solvents were commercial grade and were purchased from Fisher Scientific, Sigma-Aldrich, Santa Cruz, or Alpha Aesar. Microwave reactions were performed with a Biotage Initiator Microwave System.  $^1\text{H}$  NMR spectra were acquired on a Bruker AVANCE-400 MHz spectrometer in  $\text{CDCl}_3$  and  $\text{DMSO-}d_6$  at 25 °C. Chemical shift values are given in  $\delta$  (ppm) relatively to TMS as internal standard. Coupling constants are given in Hz. The following abbreviations are used to set multiplicities: s = singlet, d = doublet, dd= double of doublets, t = triplet, q= quartet, m = multiplet, br = broad. Mass spectrometry was done with a LTQ Orbitrap XL Hybrid Ion Trap-Orbitrap Mass Spectrometer. The molecular peaks ( $m/z$ ) was observed as  $[\text{M}+\text{H}]^+$  or  $[\text{M}-\text{H}]^-$  ions. Compounds were purified by flash chromatography using silica gel high purity grade, pore size 60 Å/230–400 mesh/particle size 40–63  $\mu\text{m}$  (Sigma-Aldrich). The final compounds were filtered through HF Bond Elut-SCX cartridges (500 mg, 6 mL, Agilent Technologies), using a 2.0 M ammonia solution in methanol (Sigma-Aldrich). LC-MS (UV and ESI-MS) and reverse-phase HPLC were used for analyzing the purity of the compounds (> 95%). Analytical LC-MS was performed on an Agilent 1200 series with UV detection at 214 and 254 nm, along with ELSD detection. General LC-MS parameters were as follow: Phenomenex-C18 Kinetex column, 50 mm  $\times$  2.1 mm, 2 min gradient, 5% (0.1% TFA/ $\text{CH}_3\text{CN}$ )/95% (0.1% TFA/ $\text{H}_2\text{O}$ ) to 100% (0.1% TFA/  $\text{CH}_3\text{CN}$ ) (all v/v). The reversed-phase HPLC system (Waters) was equipped with a dual-wavelength UV 2489 detector set at 250 and 291 nm (VNI-specific absorption maximum,  $\epsilon_{291} = 36 \text{ mM}^{-1} \text{ cm}^{-1}$ ) and a Symmetry C18 (3.5  $\mu\text{m}$ ) 4.6 mm  $\times$  75 mm column.<sup>13</sup> The mobile phase was 55% 0.015 M ammonium acetate solution (pH 7.2) and 45%  $\text{CH}_3\text{CN}$  (v/v) with an isocratic flow rate of 1.0 mL/min. The enantiomeric excess (*ee*) of the final compounds was evaluated by analytical chiral chromatography on a Chiralpak IB-3 column, 250 mm  $\times$  4.6 mm i.d. (Daicel Corporation, Japan) using a Waters HPLC system with the detector set at 250 and 291 nm. As eluent, a solution of hexane, ethanol, diethylamine, and ethylenediamine, (ratio 70:30:0.1:0.1, v/v) was used, and the flow rate was 0.7 mL/min. High resolution mass spectra were obtained on an Agilent 6540 UHD Q-TOF with ESI source. MS parameters were as follows: fragmentor: 150, capillary voltage: 3500 V, nebulizer pressure: 60 psig, drying gas flow: 13

1  
2  
3 L/min, drying gas temperature: 275° C. Samples were introduced via an Agilent 1290 UHPLC comprised of a  
4  
5 G4220A binary pump, G4226A ALS, G1316C TCC, and G4212A DAD with ULD flow cell. UV absorption was  
6  
7 observed at 215 nm and 254 nm with a 4 nm bandwidth. Column: Waters Acquity BEH C18, 1.0 x 50 mm,  
8  
9 1.7  $\mu$ m. Gradient conditions: 5% to 95% CH<sub>3</sub>CN in H<sub>2</sub>O (0.1% Formic Acid) over 1.25 min, hold at 95% CH<sub>3</sub>CN  
10  
11 for 0.25 min, 0.3 mL/min, 40° C.

### 12 13 **Preparation of (R)-1-(2,4-dichlorophenyl)-2-(1H-imidazol-1-yl)ethan-1-amine.**

14  
15 **Synthesis of 2-bromo-1-(2,4-dichlorophenyl)ethan-1-one (step 1).** CuBr<sub>2</sub> (11.8 g, 53 mmol) was ground  
16  
17 with a mortar and pestle to ensure a large surface area for the reaction and placed in a round bottom flask.  
18  
19 EtOAc (10 mL) was added and the solution was heated until reflux. Subsequently, 2',4'-  
20  
21 dichloroacetophenone (5 g, 26.5 mmol) was dissolved in CHCl<sub>3</sub> (10 mL), stirred at 40 °C, and added  
22  
23 dropwise to the CuBr<sub>2</sub> solution. The resulting mixture was stirred for 2 hours under reflux. The reaction was  
24  
25 allowed to cool at room temperature, filtrated, diluted with EtOAc, and washed with aqueous NH<sub>4</sub>Cl. The  
26  
27 organic layer was then washed with brine, dried over anhydrous Na<sub>2</sub>SO<sub>4</sub>, filtered, and the solvent removed  
28  
29 *in vacuo*. The crude product was purified by flash column chromatography (hexane/EtOAc, 8:2, v/v)  
30  
31 affording the title product as a yellow oil in quantitative yield. <sup>1</sup>H NMR (CDCl<sub>3</sub>):  $\delta$  ppm 7.56 (d, *J*= 8.4 Hz,  
32  
33 1H), 7.48 (d, *J*= 1.9 Hz, 1H), 7.36 (dd, *J*= 8.4, 1.9 Hz, 1H), 4.50 (s, 2H). ESI MS, mass calcd for C<sub>8</sub>H<sub>5</sub>BrCl<sub>2</sub>O  
34  
35 [M+H]<sup>+</sup> 267.89, found *m/z* 267.90.

36  
37  
38 **Synthesis of 1-(2,4-dichlorophenyl)-2-(1H-imidazol-1-yl)ethan-1-one (step 2).** To a solution of imidazole (9  
39  
40 g, 133 mmol) in DMF (10 mL) was added (dropwise) 2-bromo-1-(2,4-dichlorophenyl)ethan-1-one (7 g, 27  
41  
42 mmol). The reaction was stirred for 2 hours at 0 °C. The reaction mixture was diluted with H<sub>2</sub>O, extracted  
43  
44 into EtOAc, washed with LiCl (5%, w/v) and brine, and dried over anhydrous Na<sub>2</sub>SO<sub>4</sub>, filtered, and the  
45  
46 solvent was removed *in vacuo*. The crude product was purified by flash column chromatography (CH<sub>2</sub>Cl<sub>2</sub> /  
47  
48 CH<sub>3</sub>OH, 9:1, v/v) affording the title product as a white solid, isolated in 60% yield. <sup>1</sup>H NMR (CDCl<sub>3</sub>):  $\delta$  ppm  
49  
50 7.56 (d, *J*= 8.9 Hz, 1H), 7.49 (d, *J*= 1.9 Hz, 2H), 7.36 (dd, *J*= 8.4, 1.9 Hz, 1H), 7.11 (s, 1H), 6.93 (s, 1H), 5.32 (s,  
51  
52 2H). ESI MS, mass calcd for C<sub>11</sub>H<sub>8</sub>Cl<sub>2</sub>N<sub>2</sub>O [M+H]<sup>+</sup> 255.10, found *m/z* 255.3.

1  
2  
3 **Synthesis of (S)-1-(2,4-dichlorophenyl)-2-(1H-imidazol-1-yl)ethan-1-ol (step 3).** 1-(2,4-Dichlorophenyl)-2-  
4 (1H-imidazol-1-yl)ethan-1-ol was prepared as previously described using of 1-(2,4-dichlorophenyl)-2-(1H-  
5 imidazol-1-yl)ethan-1-one.<sup>28</sup> The title compound was isolated as white solid in quantitative yield. <sup>1</sup>H NMR  
6 (CDCl<sub>3</sub>): δ ppm 7.59 (d, *J* = 8.4 Hz, 1H), 7.39 (d, *J* = 2.0 Hz, 1H), 7.37 (s, 1H), 7.30 (dd, *J* = 8.4, 2.0 Hz, 1H), 6.89  
7 (s, 1H), 6.82 (s, 1H), 5.21 (dd, *J* = 8.3, 2.0 Hz, 1H), 4.19 (dd, *J* = 14.0, 2.2 Hz, 1H), 3.84 (dd, *J* = 14.0, 8.3 Hz, 1H).  
8 ESI MS, mass calcd for C<sub>11</sub>H<sub>10</sub>Cl<sub>2</sub>N<sub>2</sub>O [M+H]<sup>+</sup> 257.02, found *m/z* 256.9.

9  
10  
11 **Synthesis of (R)-1-(2-azido-2-(2,4-dichlorophenyl)ethyl)-1H-imidazole (step 4).** To a cold solution of (S)-1-  
12 (2,4-dichlorophenyl)-2-(1H-imidazol-1-yl)ethan-1-ol (230 mg, 0.9 mmol) and diphenylphosphoryl azide,  
13 (DPPA) (194 μL, 0.9 mmol) in anhydrous DMF (1.8 mL), was added dropwise 1,5-diazabicyclo[5.4.0]undec-5-  
14 ene (DBU) (188 μL, 1.26 mmol). The solution was stirred at 0 °C for 2 hours and then at room temperature  
15 overnight. Then the reaction mixture was diluted with water, extracted into EtOAc, washed with LiCl (5%,  
16 w/v) and brine, and dried over anhydrous Na<sub>2</sub>SO<sub>4</sub>, filtered, and the solvent removed *in vacuo*. The crude  
17 product was purified by flash column chromatography (CH<sub>2</sub>Cl<sub>2</sub>/CH<sub>3</sub>OH, 9:1, v/v) affording the title product  
18 as a white solid, isolated in 70% yield. <sup>1</sup>H NMR (CDCl<sub>3</sub>): δ ppm 7.43 (d, *J* = 2.0 Hz, 1H), 7.36-7.29 (m, 3H), 7.05  
19 (s, 1H), 6.90 (s, 1H), 5.24 (dd, *J* = 7.6, 3.2 Hz, 1H), 4.21 (dd, *J* = 14.4, 3.2 Hz, 1H), 4.01 (dd, *J* = 14.4, 7.6 Hz, 1H).  
20 ESI MS, mass calcd for C<sub>11</sub>H<sub>9</sub>Cl<sub>2</sub>N<sub>5</sub> [M+H]<sup>+</sup> 282.02, found *m/z* 282.0.

21  
22 **Synthesis of (R)-1-(2,4-dichlorophenyl)-2-(1H-imidazol-1-yl)ethan-1-amine (step 5).** To a suspension of  
23 LiAlH<sub>4</sub> (87.5 mg, 2.30 mmol) in dry THF (3 mL), (R)-1-(2-azido-2-(2,4-dichlorophenyl)ethyl)-1H-imidazole  
24 (542 mg, 1.92 mmol) (dissolved 2 mL of dry THF), was added dropwise at 0 °C. The suspension was warmed  
25 to room temperature and stirred overnight. The reaction mixture was quenched by Rochelle's salt and  
26 filtered through Celite. The crude product was extracted into EtOAc, washed with brine, dried on  
27 anhydrous Na<sub>2</sub>SO<sub>4</sub>, filtered, and the solvent removed *in vacuo*. The crude product was purified by flash  
28 chromatography (CH<sub>2</sub>Cl<sub>2</sub>/CH<sub>3</sub>OH, 9:1, v/v) to give a white solid in quantitative yield. <sup>1</sup>H NMR (CDCl<sub>3</sub>): δ ppm  
29 7.44-7.40 (m, 3H), 7.27 (d, *J* = 2.0 Hz, 1H), 7.06 (s, 1H), 6.90 (s, 1H), 4.72 (dd, *J* = 8.0, 3.7 Hz, 1H), 4.19 (dd, *J* =  
30 14.0, 3.7 Hz, 1H), 3.94 (dd, *J* = 14.0, 8.0 Hz, 1H). ESI MS, mass calcd for C<sub>11</sub>H<sub>11</sub>Cl<sub>2</sub>N<sub>3</sub> [M+H]<sup>+</sup> 256.03, found *m/z*  
31 256.0.

**Preparation of the side chains.** Intermediates **1b**, **2a**, **5a**, **6b**, **7a**, **8a**, and **14a** were commercially available.

**General synthesis of intermediates (3a and 4a).** To a mixture of selected acid (1 equiv.) and  $K_2CO_3$  (5 equiv.) in DMF (0.5 M) was added 2,2,2-trifluoroethyl trifluoromethanesulfonate (1.5 equiv.), and the solution was stirred at 80 °C for 2 hours. The reaction mixture was cooled to room temperature, poured into water (100 mL), and the aqueous layer was extracted by EtOAc, washed with brine, dried with anhydrous  $Na_2SO_4$ , and filtered, and the solvent removed *in vacuo*. The crude product was purified by flash chromatography ( $CH_2Cl_2/CH_3OH$ , 9:1) to give a white solid.

**2-Fluoro-4-(2,2,2-trifluoroethoxy)benzoic acid (3a).** Yield 78%.  $^1H$  NMR ( $DMSO-d_6$ )  $\delta$  11.0 (br, 1H), 7.77 (t,  $J = 8.8$  Hz, 1H), 6.73 (dd,  $J = 8.7, 2.3$  Hz, 1H), 6.65 (dd,  $J = 13.1, 2.2$  Hz, 1H), 4.90 (q,  $J = 8.8$  Hz, 2H). ESI MS, mass calcd for  $C_9H_6F_4O_3$   $[M-H]^-$  237.03, found  $m/z$  236.9.

**3-Fluoro-5-(2,2,2-trifluoroethoxy)benzoic acid (4a).** Yield 50%.  $^1H$  NMR ( $DMSO-d_6$ )  $\delta$  11.0 (br, 1H), 7.20 (s, 1H), 7.07 (d,  $J = 8.8$  Hz, 1H), 6.90 (d,  $J = 10.6$  Hz, 1H), 4.92 (q,  $J = 9.0$  Hz, 2H). ESI MS, mass calcd for  $C_9H_6F_4O_3$   $[M-H]^-$  237.03, found  $m/z$  237.0.

**General synthesis of intermediates (9a-13a).** The selected boronic acid (1 equiv.), 2-bromopyridine (1 equiv.), [1,1'-bis(diphenylphosphino)ferrocene]dichloropalladium(II) ( $Pd(dppf)Cl_2$ ) (0.6 mol%), dioxane, and  $H_2O$  (ratio 4:1, v/v) were stirred under argon. The reaction was performed in the microwave reactor for 30 min at 120 °C. The solvent was evaporated, and the crude residue was extracted with EtOAc, washed with brine, and dried over anhydrous  $Na_2SO_4$ , filtered, and the solvent removed *in vacuo*. The crude product was purified by flash chromatography (hexanes/EtOAc, 4:1, v/v) to give a white solid in 50-70% yield.

**Methyl 3-(pyridin-2-yl)benzoate (9a).** Yield 60%.  $^1H$  NMR ( $CDCl_3$ ):  $\delta$  ppm 8.74-8.72 (m, 1H), 8.65-8.64 (m, 1H), 8.27-8.24 (m, 1H), 8.11-8.09 (m, 1H), 7.80 (m, 2H), 7.57 (t,  $J = 7.8$  Hz, 1H), 7.30-7.27 (m, 1H), 3.96 (s, 3H). ESI MS, mass calcd for  $C_{13}H_{11}NO_2$   $[M+H]^+$  214.08, found  $m/z$  214.10.

**Methyl 4-(pyridin-2-yl)benzoate (10a).** Yield 50%.  $^1H$  NMR ( $CDCl_3$ ):  $\delta$  ppm 8.74-8.72 (m, 1H), 8.15 (d,  $J = 8.6$  Hz, 2H), 8.08 (d,  $J = 8.6$  Hz, 2H), 7.80-7.79 (m, 2H), 7.31-7.28 (m, 1H), 3.95 (s, 3H). ESI MS, mass calcd for  $C_{13}H_{11}NO_2$   $[M+H]^+$  214.08, found  $m/z$  214.05.

**Methyl 3-fluoro-5-(pyridin-2-yl)benzoate (11a).** Yield 70%.  $^1\text{H NMR}$  ( $\text{CDCl}_3$ ):  $\delta$  ppm 8.73-8.72 (m, 1H), 8.45-8.44 (m, 1H), 8.03-7.99 (m, 1H), 7.82-7.75 (m, 3H), 7.33-7.30 (m, 1H), 3.97 (s, 3H). ESI MS, mass calcd for  $\text{C}_{13}\text{H}_{10}\text{FNO}_2$   $[\text{M}+\text{H}]^+$  232.07, found  $m/z$  232.1.

**Methyl 2-fluoro-4-(pyridin-2-yl)benzoate (12a).** Yield 50 %.  $^1\text{H NMR}$  ( $\text{CDCl}_3$ ):  $\delta$  ppm 8.73-8.71 (m, 1H), 8.05-7.95 (m, 1H), 7.86 (s, 1H), 7.84-7.76 (m, 3H), 7.34-7.31 (m, 1H), 3.96 (s, 3H). ESI MS, mass calcd for  $\text{C}_{13}\text{H}_{10}\text{FNO}_2$   $[\text{M}+\text{H}]^+$  232.07, found  $m/z$  232.1.

**Methyl 2-fluoro-5-(pyridin-2-yl)benzoate (13a).** Yield 60 %.  $^1\text{H NMR}$  ( $\text{CDCl}_3$ ):  $\delta$  ppm 8.69-8.67 (m, 1H), 8.54 (dd,  $J=9.4, 2.5$  Hz, 1H), 8.23-8.19 (m, 1H), 7.79-7.72 (m, 2H), 7.27-7.26 (m, 1H), 7.24 (d,  $J=1.5$  Hz, 1H), 3.96 (s, 3H). ESI MS, mass calcd for  $\text{C}_{13}\text{H}_{10}\text{FNO}_2$   $[\text{M}+\text{H}]^+$  232.07, found  $m/z$  232.09.

**Methyl 3-fluoro-5-(5-fluoropyrimidin-4-yl)benzoate (15a).** Yield 92 %.  $^1\text{H NMR}$  ( $\text{CDCl}_3$ ):  $\delta$  ppm 9.13 (d,  $J=3.0$  Hz), 8.72 (s, 1H), 8.65 (s, 1H), 8.12-8.09 (m, 1H), 7.91-7.88 (m, 1H), 3.4 (s, 3H). ESI MS, mass calcd for  $\text{C}_{12}\text{H}_8\text{F}_2\text{N}_2\text{O}_2$   $[\text{M}+\text{H}]^+$  251.06, found  $m/z$  251.10.

**General synthesis of intermediates b and c.** To a solution of substituted benzoic acid (1 equiv.) in EtOH, hydrazine monohydrate (2 equiv.) and few drops of concentrated  $\text{H}_2\text{SO}_4$  were added. The reaction mixture was heated under reflux for 6 hours and then, after cooling, the white solid was filtered to give desired product (**intermediate b**) in quantitative yield, which was used for the next step. (The same procedure was performed with substituted methyl benzoate without adding concentrated  $\text{H}_2\text{SO}_4$ ).

Subsequently, methyl 4-(chlorocarbonyl)benzoate, dissolved in anhydrous THF, was added dropwise to a dried round bottom flask containing the appropriate **intermediate b**, under an argon flow. The mixture was stirred at room temperature for 6 hours. Then the solvent was removed under reduced pressure. The corresponding  $N'$ -benzoyl-(hydrazinocarbonyl)esters, differently substituted, were used without further purification in the next step, when  $\text{POCl}_3$  was added dropwise. The mixture was heated at reflux overnight (85 °C), then cooled to room temperature and poured into ice and solid  $\text{NaHCO}_3$ . The resulting solution was extracted with EtOAc, washed with  $\text{H}_2\text{O}$ , and dried with  $\text{Na}_2\text{SO}_4$ . Differently substituted methyl 4-(5-phenyl-1,3,4-oxadiazol-2-yl)benzoates were purified by flash chromatography (hexane/EtOAc, 3:1, v/v). The hydrolysis of the benzoate ester to benzoic acid was performed by adding, to

1  
2  
3 a suspension of the benzoate in THF, LiOH·H<sub>2</sub>O and CH<sub>3</sub>OH (THF/CH<sub>3</sub>OH /H<sub>2</sub>O, 3:1:1, v/v/v). The reaction  
4  
5 mixture was stirred at room temperature for 3 hours, and then the solvent was removed under reduced  
6  
7 pressure, and the residue was extracted with an aqueous HCl solution and EtOAc. The solvent was  
8  
9 evaporated and a white pure solid was obtained in quantitative yield (**intermediate c**).

10  
11 **General Procedure for amide coupling (step 6).** (*R*)-1-(2,4-Dichlorophenyl)-2-(1*H*-imidazol-1-yl)ethan-1-  
12  
13 amine (1.2 equiv.) was dissolved in CH<sub>2</sub>Cl<sub>2</sub> (4 mL) and the corresponding acid (**intermediate c**, 1.0 equiv.)  
14  
15 was added to the round bottom flask, which was cooled to 0 °C before adding *N*-(3-dimethylaminopropyl)-  
16  
17 *N*'-ethylcarbodiimide hydrochloride (EDC/HCl) (1.0 equiv.) and 4-dimethylaminopyridine (DMAP). The  
18  
19 reaction mixture was warmed to room temperature and stirred overnight. The mixture was diluted with  
20  
21 CH<sub>2</sub>Cl<sub>2</sub>, washed with NaHCO<sub>3</sub>, and brine dried on Na<sub>2</sub>SO<sub>4</sub>. The solvent was evaporated and the final  
22  
23 compound was purified by flash chromatography (CH<sub>2</sub>Cl<sub>2</sub>/CH<sub>3</sub>OH, 9:1, v/v). The yields were calculated as  
24  
25 pure compounds, obtained as a white solid.

26  
27  
28 **(*R*)-*N*-(1-(2,4-Dichlorophenyl)-2-(1*H*-imidazol-1-yl)ethyl)-4-(5-(3,4-difluorophenyl)-1,3,4-oxadiazol-2-  
29  
30 yl)benzamide (compound 1).** Yield 50 %. <sup>1</sup>H NMR (CDCl<sub>3</sub>): δ ppm 9.97 (s, 1H), 9.55 (d, *J*= 8.8 Hz, 1H), 8.04 (d,  
31  
32 *J*= 8.4 Hz, 2H), 7.98-7.89 (m, 2H), 7.79 (dd, *J*= 8.3, 5.2 Hz, 3H), 7.47-7.45 (m, 2H), 7.40-7.35 (m, 3H), 6.08-  
33  
34 6.04 (m, 1H), 5.27 (dd, *J*= 13.8, 12.0 Hz, 1H), 4.41 (dd, *J*= 14.0, 3.2 Hz, 1H). LC-MS, found [M+H]<sup>+</sup> *m/z* 539.8;  
35  
36 ESI MS, mass calcd for C<sub>26</sub>H<sub>17</sub>Cl<sub>2</sub>F<sub>2</sub>N<sub>5</sub>O<sub>2</sub> [M]<sup>+</sup> 539.0727, found *M*<sub>obs</sub> 539.0733. HPLC, *t*<sub>R</sub> 12.6 min, purity 98 %.  
37  
38 Enantiomeric excess > 97 %.

39  
40  
41 **(*R*)-*N*-(1-(2,4-Dichlorophenyl)-2-(1*H*-imidazol-1-yl)ethyl)-4-(5-(3-fluoro-4-(trifluoromethyl)phenyl)-1,3,4-  
42  
43 oxadiazol-2-yl)benzamide (compound 2).** Yield 50 %. <sup>1</sup>H NMR (CDCl<sub>3</sub>): δ ppm 9.92 (s, 1H), 9.49 (d, *J*= 8.5 Hz,  
44  
45 1H), 8.08 (d, *J*= 8.4 Hz, 2H), 8.04 (d, *J*= 8.2 Hz, 1H), 7.97 (d, *J*= 10.2 Hz, 1H), 7.82-7.77 (m, 4H), 7.47-7.45 (m,  
46  
47 2H), 7.40 (s, 1H), 7.35 (dd, *J*= 8.4, 2.0 Hz, 1H), 6.09-6.04 (m, 1H), 5.26 (dd, *J*= 14.0, 12.0 Hz, 1H), 4.42 (dd, *J*=  
48  
49 14.0, 3.3 Hz, 1H). LC-MS found, [M+H]<sup>+</sup> *m/z* 590.18; ESI MS, mass calcd for C<sub>27</sub>H<sub>17</sub>Cl<sub>2</sub>F<sub>4</sub>N<sub>5</sub>O<sub>2</sub> [M]<sup>+</sup> 598.0695,  
50  
51 found *M*<sub>obs</sub> 598.0696. HPLC, *t*<sub>R</sub> 11.4 min, purity 99 %. Enantiomeric excess > 97 %.

52  
53 **(*R*)-*N*-(1-(2,4-Dichlorophenyl)-2-(1*H*-imidazol-1-yl)ethyl)-4-(5-(2-fluoro-4-(2,2,2-trifluoroethoxy)phenyl)-  
54  
55 1,3,4-oxadiazol-2-yl)benzamide (compound 3).** Yield 40 %. <sup>1</sup>H NMR (CDCl<sub>3</sub>): δ ppm 9.79 (s, 1H), 9.47 (d,  
56  
57



1  
2  
3  $J=8.4$  Hz, 1H), 8.13 (t,  $J= 8.4$  Hz, 1H), 8.02 (d,  $J= 8.3$  Hz, 2H), 7.80 (dd,  $J= 8.3, 3.4$  Hz, 3H), 7.45 (d,  $J= 2.0$  Hz,  
4 1H), 7.44 (s, 1H), 7.38 (s, 1H), 7.34 (dd,  $J= 8.4, 2.0$  Hz, 1H), 6.94-6.86 (m, 2H), 6.07-6.02 (m, 1H), 5.23 (dd,  $J=$   
5 13.6, 12.4 Hz, 1H), 4.49-4.39 (m, 3H). LC-MS, found  $[M+H]^+$   $m/z$  618.10; ESI MS, mass calcd for  
6  $C_{28}H_{19}Cl_2F_4N_5O_3$   $[M]^+$  619.0801, found  $M_{obs}$  619.0805. HPLC,  $t_R$  17.6 min, purity 99 %. Enantiomeric excess >  
7 97 %.

8  
9  
10  
11  
12  
13 **(R)-N-(1-(2,4-Dichlorophenyl)-2-(1H-imidazol-1-yl)ethyl)-4-(5-(3-fluoro-5-(2,2,2-trifluoroethoxy)phenyl)-**  
14 **1,3,4-oxadiazol-2-yl)benzamide (compound 4)** . Yield 30 %.  $^1H$  NMR ( $CDCl_3$ ):  $\delta$  ppm 10.0 (s, 1H), 9.55 (d,  $J=$   
15 9.0 Hz, 1H), 8.04 (d,  $J= 8.3$  Hz, 2H), 7.78 (dd,  $J= 11.4, 8.4$  Hz, 3H), 7.55-7.53 (m, 2H), 7.46-7.45 (m, 2H), 7.42  
16 (s, 1H), 7.36 (dd,  $J= 8.4, 2.0$  Hz, 1H), 6.93-6.90 (m, 1H), 6.08-6.04 (m, 1H), 5.30 (dd,  $J= 14.0, 11.8$  Hz, 1H),  
17 4.49-4.45 (m, 2H), 4.42-4.38 (m, 1H). LC-MS, found  $[M+H]^+$   $m/z$  620.09; ESI MS, mass calcd for  
18  $C_{28}H_{19}Cl_2F_4N_5O_3$   $[M]^+$  619.0801, found  $M_{obs}$  619.0802. HPLC,  $t_R$  13.4 min, purity 98 %. Enantiomeric excess >  
19 97 %.

20  
21  
22  
23  
24  
25  
26  
27  
28 **(R)-4-(5-(3,4-Dichlorophenyl)-1,3,4-oxadiazol-2-yl)-N-(1-(2,4-dichlorophenyl)-2-(1H-imidazol-1-**  
29 **yl)ethyl)benzamide (compound 5)**. Yield 20%.  $^1H$  NMR ( $CDCl_3$ ):  $\delta$  ppm 8.21 (br, 1H), 8.16 (d,  $J= 2.0$  Hz, 1H),  
30 8.04 (d,  $J= 8.4$  Hz, 2H), 7.96 (d,  $J= 8.4$  Hz, 2H), 7.93 (dd,  $J= 8.4, 2.0$  Hz, 1H), 7.61 (d,  $J= 8.4$  Hz, 1H), 7.45 (d,  $J=$   
31 2.0 Hz, 1H), 7.42 (d,  $J= 8.4$  Hz, 1H), 7.23 (dd,  $J= 8.4, 2.0$  Hz, 1H), 7.09 (s, 1H), 7.05 (s, 1H), 5.92-5.87 (m, 1H),  
32 4.76 (dd,  $J= 14.0, 8.9$  Hz, 1H), 4.26 (dd,  $J= 14.0, 5.1$  Hz, 1H). LC-MS, found  $[M+H]^+$   $m/z$  573.91; ESI MS, mass  
33 calcd for  $C_{26}H_{17}Cl_4N_5O_2$   $[M]^+$  571.1036, found  $M_{obs}$  571.1046. HPLC,  $t_R$  13.4 min, purity 98 %. Enantiomeric  
34 excess > 97 %.

35  
36  
37  
38  
39  
40  
41  
42  
43 **(R)-4-(5-(3-Bromophenyl)-1,3,4-oxadiazol-2-yl)-N-(1-(2,4-dichlorophenyl)-2-(1H-imidazol-1-**  
44 **yl)ethyl)benzamide (compound 6)**. Yield 50%.  $^1H$  NMR ( $CDCl_3$ ):  $\delta$  ppm 8.30 (s, 1H), 8.24 (d,  $J= 7.4$  Hz, 2H),  
45 8.11 (d,  $J= 7.5$  Hz, 1H), 7.91 (d,  $J= 7.5$  Hz, 2H), 7.72 (d,  $J= 7.8$  Hz, 1H), 7.51 (s, 1H), 7.45 (m, 1H), 7.35 (s, 1H),  
46 7.12 (d,  $J= 7.8$  Hz, 1H), 7.06 (s, 1H), 6.95-6.93 (m, 1H), 6.86 (s, 1H), 5.79 (m, 1H), 4.56 (d,  $J= 6.48$  Hz, 2H). LC-  
47 MS, found  $[M+H]^+$   $m/z$  581.9; ESI MS, mass calcd for  $C_{26}H_{18}BrCl_2N_5O_2$   $[M]^+$  581.0021, found  $M_{obs}$  581.0026.  
48 HPLC,  $t_R$  17.0 min, purity 98 %. Enantiomeric excess > 97 %.

1  
2  
3 **(R)-N-(1-(2,4-Dichlorophenyl)-2-(1H-imidazol-1-yl)ethyl)-4-(5-(3-morpholinophenyl)-1,3,4-oxadiazol-2-**  
4 **yl)benzamide (compound 7).** Yield 60%. <sup>1</sup>H NMR (CDCl<sub>3</sub>): δ ppm 8.06 (d, *J* = 7.6 Hz, 2H), 7.91 (d, *J* = 7.6 Hz,  
5 1H), 7.87 (d, *J* = 7.6 Hz, 2H), 7.60 (s, 1H) 7.53 (d, *J* = 7.0 Hz, 1H), 7.45 (s, 1H), 7.41-7.29 (m, 3H), 7.22 (d, *J* = 8.2  
6 Hz, 1H), 7.08 (d, *J* = 7.5 Hz, 1H), 7.0 (s, 1H), 6.92 (s, 1H), 5.88-5.79 (m, 1H), 4.55 (dd, *J* = 13.7, 6.8 Hz, 1H), 4.45  
7 (dd, *J* = 13.0, 4.4 Hz, 1H), 3.87 (s, 4H), 3.22 (s, 4H). LC-MS, found [M+H]<sup>+</sup> *m/z* 589.6. HPLC, *t*<sub>R</sub> 7.3 min, purity  
8 98 %. Enantiomeric excess > 97 %.

9  
10  
11 **(R)-N-(1-(2,4-Dichlorophenyl)-2-(1H-imidazol-1-yl)ethyl)-4-(5-(4-morpholinophenyl)-1,3,4-oxadiazol-2-**  
12 **yl)benzamide (compound 8).** Yield 40 %. <sup>1</sup>H NMR (CDCl<sub>3</sub>): δ ppm 8.27 (br, 1H), 8.04 (d, *J* = 8.2 Hz, 2H), 7.98-  
13 7.95 (m, 4H), 7.48 (s, 1H), 7.45 (d, *J* = 2.0 Hz, 2H), 7.24 (dd, *J* = 8.4, 2.0 Hz, 1H), 7.08 (br, 2H), 6.97 (s, 1H), 6.95  
14 (s, 1H), 5.95-5.90 (m, 1H), 4.79 (dd, *J* = 13.2, 8.1 Hz, 1H), 4.45 (dd, *J* = 14.0, 4.4 Hz, 1H), 3.87 (m, 4H), 3.22 (m,  
15 4H). LC-MS, found [M+H]<sup>+</sup> *m/z* 589.23. HPLC, *t*<sub>R</sub> 6.8 min, purity 98 %. Enantiomeric excess > 97 %.

16  
17 **(R)-N-(1-(2,4-Dichlorophenyl)-2-(1H-imidazol-1-yl)ethyl)-4-(5-(3-(pyridin-2-yl)phenyl)-1,3,4-oxadiazol-2-**  
18 **yl)benzamide (compound 9).** Yield 20 %. <sup>1</sup>H NMR (CDCl<sub>3</sub>): δ ppm 8.75-8.74 (m, 2H), 8.48 (s, 1H), 8.38 (s,  
19 1H), 8.21-8.18 (m, 2H), 8.04 (d, *J* = 8.4 Hz, 2H), 7.99 (d, *J* = 8.4 Hz, 2H), 7.84-7.82 (m, 2H), 7.65 (t, *J* = 7.8 Hz,  
20 1H), 7.50 (d, *J* = 8.6 Hz, 1H), 7.44 (d, *J* = 2.0 Hz, 1H), 7.33-7.30 (m, 1H), 7.28 (d, *J* = 2.2 Hz, 1H), 7.20 (s, 1H),  
21 5.96-5.90 (m, 1H), 4.89 (dd, *J* = 14.0, 9.5 Hz, 1H), 4.46 (dd, *J* = 14.0, 4.9 Hz, 1H). (One signal was overlapped  
22 with CDCl<sub>3</sub>). LC-MS, found [M+H]<sup>+</sup> *m/z* 581.2; ESI MS, mass calcd for C<sub>31</sub>H<sub>22</sub>Cl<sub>2</sub>N<sub>6</sub>O<sub>2</sub> [M]<sup>+</sup> 580.1181, found  
23 *M*<sub>obs</sub> 580.1192. HPLC, *t*<sub>R</sub> 11.0 min, purity 99 %. Enantiomeric excess > 97 %.

24  
25  
26 **(R)-N-(1-(2,4-Dichlorophenyl)-2-(1H-imidazol-1-yl)ethyl)-4-(5-(4-(pyridin-2-yl)phenyl)-1,3,4-oxadiazol-2-**  
27 **yl)benzamide (compound 10).** Yield 30 %. <sup>1</sup>H NMR (CDCl<sub>3</sub>): δ ppm 8.75 (d, *J* = 4.5 Hz, 1H), 8.67-8.62 (m, 2H),  
28 8.23-8.17 (m, 4H), 8.05 (s, 3H), 7.82-7.81 (m, 2H), 7.58 (d, *J* = 8.4 Hz, 1H), 7.46 (d, *J* = 2.0 Hz, 1H), 7.33-7.28  
29 (m, 2H), 7.19 (s, 2H), 6.00-5.95 (m, 1H), 4.95 (dd, *J* = 14.0, 9.6 Hz, 1H), 4.45 (dd, *J* = 14.0, 4.4 Hz, 1H). (One  
30 signal is overlapped with CDCl<sub>3</sub>). LC-MS, found [M+H]<sup>+</sup> *m/z* 581.09; ESI MS, mass calcd for C<sub>31</sub>H<sub>22</sub>Cl<sub>2</sub>N<sub>6</sub>O<sub>2</sub>  
31 [M]<sup>+</sup> 580.1181, found *M*<sub>obs</sub> 580.1195. HPLC, *t*<sub>R</sub> 10.9 min, purity 99 %. Enantiomeric excess > 97 %.

32  
33  
34 **(R)-N-(1-(2,4-Dichlorophenyl)-2-(1H-imidazol-1-yl)ethyl)-4-(5-(3-fluoro-5-(pyridin-2-yl)phenyl)-1,3,4-**  
35 **oxadiazol-2-yl)benzamide (compound 11).** Yield 20 %. <sup>1</sup>H NMR (CDCl<sub>3</sub>): δ ppm 10 (s, 1H), 9.58 (d, *J* = 8.7 Hz,

1  
2  
3 1H), 8.75 (d,  $J = 4.6$  Hz, 1H), 8.59 (s, 1H), 8.04 (d,  $J = 8.4$  Hz, 2H), 7.88-7.86 (m, 2H), 7.82-7.75 (m, 4H), 7.69 (s,  
4 1H), 7.46 (s, 1H), 7.42 (d,  $J = 2.0$  Hz, 1H), 7.38-7.32 (m, 3H), 6.09-6.03 (m, 1H), 5.30 (dd,  $J = 13.4, 12.0$  Hz, 1H),  
5 4.41 (dd,  $J = 13.6, 3.0$  Hz, 1H). LC-MS, found  $[M+H]^+$   $m/z$  599.09; ESI MS, mass calcd for  $C_{31}H_{21}Cl_2FN_6O_2$   
6  
7  $[M+H]^+$  598.1087, found  $M_{obs}$  5998.1092. HPLC,  $t_R$  8.5 min, purity 98 %. Enantiomeric excess > 97 %.

8  
9  
10  
11 **(R)-N-(1-(2,4-Dichlorophenyl)-2-(1H-imidazol-1-yl)ethyl)-4-(5-(4-(3-fluoropyridin-2-yl)phenyl)-1,3,4-**

12 **oxadiazol-2-yl)benzamide (compound 12).** Yield 40 %.  $^1H$  NMR ( $CDCl_3$ ):  $\delta$  ppm 10.0 (s, 1H), 9.55 (d,  $J = 8.7$   
13 Hz, 1H), 8.76 (d,  $J = 4.6$  Hz, 1H), 8.28 (t,  $J = 7.8$  Hz, 1H), 8.05-8.01 (m, 3H), 7.98 (dd,  $J = 8.2, 1.4$  Hz, 1H), 7.86-  
14 7.77 (m, 5H), 7.52 (s, 1H), 7.44 (d,  $J = 2.0$  Hz, 2H), 7.38-7.33 (m, 2H), 6.09-6.03 (m, 1H), 5.24 (dd,  $J = 13.8,$   
15 12.5 Hz, 1H), 4.43 (dd,  $J = 14.0, 3.2$  Hz, 1H). LC-MS, found  $[M+H]^+$   $m/z$  599.14; ESI MS, mass calcd for  
16  $C_{28}H_{19}Cl_2F_4N_5O_3$   $[M]^+$  619.0801, found  $M_{obs}$  619.0802. HPLC,  $t_R$  6.2 min, purity 99 %. Enantiomeric excess >  
17 97 %.

18  
19  
20  
21 **(R)-N-(1-(2,4-Dichlorophenyl)-2-(1H-imidazol-1-yl)ethyl)-4-(5-(2-fluoro-5-(pyridin-2-yl)phenyl)-1,3,4-**

22 **oxadiazol-2-yl)benzamide (compound 13).** Yield 20 %.  $^1H$  NMR ( $CDCl_3$ ):  $\delta$  ppm 10.0 (s, 1H), 9.77 (d,  $J = 9.6$   
23 Hz, 1H), 8.96 (d,  $J = 5.6$  Hz, 1H), 8.90 (dd,  $J = 6.0, 2.2$  Hz, 1H), 8.45-8.41 (m, 1H), 8.35-8.30 (m, 1H), 8.18 (d,  $J =$   
24 8.4 Hz, 1H), 8.07 (d,  $J = 8.3$  Hz, 2H), 8.01 (s, 1H), 7.86 (dd,  $J = 8.4, 4.0$  Hz, 3H), 7.53-7.50 (m, 2H), 7.46 (s, 1H),  
25 7.42 (d,  $J = 2.0$  Hz, 1H), 7.33 (dd,  $J = 8.5, 2.0$  Hz, 1H), 6.09-6.03 (m, 1H), 5.34 (dd,  $J = 13.8, 12.5$  Hz, 1H), 4.43  
26 (dd,  $J = 13.2, 2.5$  Hz, 1H). LCMS, found  $[M+H]^+$   $m/z$  599.18; ESI MS, mass calcd for  $C_{31}H_{21}Cl_2FN_6O_2$   $[M]^+$   
27 598.1087, found  $M_{obs}$  598.1090. HPLC,  $t_R$  10.3 min, purity 99 %. Enantiomeric excess > 97 %.

28  
29  
30  
31 **(R)-4-(5-(3-Chloro-4-(methylsulfonyl)phenyl)-1,3,4-oxadiazol-2-yl)-N-(1-(2,4-dichlorophenyl)-2-(1H-**

32 **imidazol-1-yl)ethyl)benzamide (compound 14).** Yield 50 %.  $^1H$  NMR ( $CDCl_3$ ):  $\delta$  ppm 10.0 (s, 1H), 9.57 (d,  $J =$   
33 8.6 Hz, 1H), 8.35 (s, 1H), 8.34-8.33 (m, 1H), 8.22 (dd,  $J = 8.2, 1.5$  Hz, 1H), 8.07 (d,  $J = 8.3$  Hz, 2H) 7.78 (dd,  $J =$   
34 8.2, 5.04 Hz, 3H), 7.50 (s, 1H), 7.47 (d,  $J = 2.0$  Hz, 1H), 7.44 (s, 1H), 6.10-6.05 (m, 1H), 5.30 (dd,  $J = 13.8, 12.4$   
35 Hz, 1H), 4.42 (dd,  $J = 13.6, 2.6$  Hz, 1H), 3.35 (s, 3H). LC-MS, found  $[M+H]^+$   $m/z$  617.7; ESI MS, mass calcd for  
36  $C_{27}H_{20}Cl_3N_5O_4S$   $[M]^+$  6175.0302, found  $M_{obs}$  615.0315. HPLC,  $t_R$  5.8 min, purity 99 %. Enantiomeric excess >  
37 97 %.

1  
2  
3 **(R)-N-(1-(2,4-Dichlorophenyl)-2-(1H-imidazol-1-yl)ethyl)-4-(5-(3-fluoro-5-(5-fluoropyrimidin-4-yl)phenyl)-**  
4 **1,3,4-oxadiazol-2-yl)benzamide (compound 15).** Yield 30 %. <sup>1</sup>H NMR (CDCl<sub>3</sub>): δ ppm 10.04 (s, 1H), 9.54 (d,  
5 *J*= 8.7 Hz, 1H), 9.16 (d, *J*= 3.0 Hz, 1H), 8.76 (d, *J*= 3.4 Hz, 1H), 8.73 (s, 1H), 8-11-8.08 (m, 1H), 8.06 (d, *J*= 8.5  
6 Hz, 2H), 8.02-7.99 (m, 1H), 7.80 (dd, *J*= 8.4, 3.0 Hz, 3H), 7.55 (s, 1H), 7.45 (d, *J*= 2.0 Hz, 2H), 7.35 (dd, *J*= 8.4,  
7 2.0 Hz, 1H), 6.09-6.03 (m, 1H), 5.30 (dd, *J*= 14.0, 12.0 Hz, 1H), 4.42 (dd, *J*= 14.0, 3.0 Hz). LC-MS, found  
8 [M+H]<sup>+</sup> *m/z* 617.8; ESI MS, mass calcd for C<sub>30</sub>H<sub>19</sub>Cl<sub>2</sub>F<sub>2</sub>N<sub>7</sub>O<sub>2</sub> [M]<sup>+</sup> 617.0945, found *M*<sub>obs</sub> 617.0949. HPLC, *t*<sub>R</sub>  
9 13.0 min, purity 99 %. Enantiomeric excess > 97 %.

10  
11  
12  
13  
14  
15  
16  
17  
18  
19 **CYP51 activity assay.** *A. fumigatus* and *C. albicans* CYP51 were expressed in *Escherichia coli* and purified  
20 as described earlier.<sup>9-10</sup> The enzymatic reaction mixture contained 0.5 μM *A. fumigatus*<sup>9</sup> or *C. albicans*<sup>10</sup>  
21 CYP51 and 1.0 μM rat NADPH-cytochrome P450 reductase, 100 μM L-α-1,2-dilauroyl-*sn*-  
22 glycerophosphocholine, 0.4 mg/mL isocitrate dehydrogenase, and 25 mM sodium isocitrate in 50 mM  
23 potassium phosphate buffer (pH 7.2) containing 10% glycerol (v/v) and 0.1% Triton X-100 (v/v). After  
24 addition of the radiolabeled ([3-<sup>3</sup>H]) sterol substrate (eburicol for *A. fumigatus* and lanosterol for *C.*  
25 *albicans* CYP51), final concentration 25 μM, and an inhibitor, final concentration 0.75 μM, the mixture was  
26 preincubated for 60 seconds at 37 °C in a shaking water bath, and the reaction was initiated by the addition  
27 of 100 μM NADPH and stopped by extraction of the sterols with EtOAc. The extracted sterols were dried,  
28 dissolved in CH<sub>3</sub>OH, and analyzed using a reversed-phase HPLC system (Waters) equipped with a β-RAM  
29 detector (INUS Systems, Inc.) using a NovaPak octadecylsilane (C<sub>18</sub>) column (particle size 4 μm, 3.9 mm ×  
30 150 mm) and a linear gradient of H<sub>2</sub>O, CH<sub>3</sub>CN, and CH<sub>3</sub>OH.<sup>9-10</sup> The inhibitory potencies of VNI and  
31 derivatives were compared as percentage of inhibition of sterol 14α-demethylation in 60-min reactions;<sup>16, 18</sup>  
32 the molar ratio inhibitor/enzyme/substrate in the reaction mixture was 1.5:1:50. Two clinical systemic  
33 antifungal drugs, fluconazole and posaconazole, were used as controls. The experiments were performed in  
34 triplicate, and the results are presented as means ± SD.

**CYP51 ligand binding assay.** Spectral titrations of *C. albicans* and *A. fumigatus* CYP51 with selected VNI derivatives were carried out in 5 cm optical path length cuvettes at 0.5  $\mu\text{M}$  P450 concentration as previously described.<sup>15</sup> The ligands were added from 0.2 mM stock solutions in DMSO, and the titration range was 0.1-0.8  $\mu\text{M}$ . The apparent dissociation constants of the enzyme-inhibitor complex were calculated as red shifts in the P450 Soret band maximum (from 417 to 424 nm<sup>29</sup>) using GraphPad Prism 6 software by fitting the data for the ligand-induced absorbance changes in the difference spectra  $\Delta(A_{\text{max}} - A_{\text{min}})$  versus ligand concentration to the quadratic equation 1 (tight-binding ligands),<sup>14</sup>

$$\Delta A = (\Delta A_{\text{max}} / 2E) \left( (L + E + K_d) - \sqrt{(L + E + K_d)^2 - 4LE} \right)^{0.5} \quad (\text{Eq.1})$$

where [L] and [E] are the total concentrations of ligand and enzyme used for the titration, respectively.

**Microsomal stability assay. Intrinsic clearance in hepatic microsomes** (human, rat, mouse). Human (mixed gender), rat (male Sprague-Dawley), or mouse (male CD-1) pooled liver microsomes (0.5 mg/mL, BD Biosciences) and 1  $\mu\text{M}$  test compound were incubated in 100 mM potassium phosphate buffer (pH 7.4) with 3 mM  $\text{MgCl}_2$  at 37 °C with constant shaking. After a 5 min preincubation, each reaction was initiated by the addition of 1 mM NADPH. At selected time intervals (0, 3, 7, 15, 25, and 45 min), 50  $\mu\text{L}$  aliquots were taken and subsequently placed into a 96-well plate containing 150  $\mu\text{L}$  of cold  $\text{CH}_3\text{CN}$  with internal standard (50 ng/mL carbamazepine). Plates were then centrifuged at 3000 g (4 °C) for 10 min, and the supernatants were transferred to a separate 96-well plate and diluted 1:1 (v/v) with  $\text{H}_2\text{O}$  for LC/MS/MS analysis. The experiments were performed in triplicate. The *in vitro* half-life ( $T_{1/2}$ , min, Eq. 1), estimated intrinsic clearance ( $\text{CL}_{\text{INT}}$ , mL/min/kg, Eq. 2) and subsequent predicted hepatic clearance ( $\text{CL}_{\text{HEP}}$ , mL/min/kg, Eq. 3) were determined employing the following equations:

$$T_{1/2} = \frac{\ln(2)}{k} \quad (1)$$

where  $k$  represents the slope from linear regression analysis of the natural log percent remaining of test compound as a function of incubation time

$$\text{CL}_{\text{int}} = \frac{0.693}{\text{in vitro } T_{1/2}} \times \frac{\text{mL incubation}}{\text{mg microsomes}} \times \frac{45 \text{ mg microsomes}}{\text{gram liver}} \times \frac{45^{\text{g}} \text{ gram liver}}{\text{Kg body wt}} \quad (2)$$

<sup>a</sup>scaling factor

$$CL_{\text{hep}} = \frac{Q_h \cdot CL_{\text{int}}}{Q_h + CL_{\text{int}}} \quad (3)$$

where  $Q_h$  (hepatic blood flow) is 21 mL/min/kg for human, 70 mL/min/kg for rat, and 90 mL/min/kg for mouse.

**Antifungal drug susceptibility test.** The Minimal Inhibitory Concentration (MIC) of each drug against the various *A. fumigatus* strains was investigated using the Clinical and Laboratory Standards Institute broth microdilution method, document M38-A2.<sup>30</sup> The tests were performed in triplicate. Various strains of *A. fumigatus*, 1022, 32820, and MYA626 (ATCC<sup>®</sup> MP-12 kit), were grown according to the protocol.<sup>30</sup> Briefly, the strains were initially plated onto potato dextrose agarose plates for 5 to 6 days at 35 °C to generate conidia. The agar plate surfaces were washed with 5 mL of sterile 1x phosphate-buffered saline with 0.05% Tween-80 (v/v) to obtain the independent conidia, and the number of conidia were counted with a hemocytometer. The conidia were further diluted in RPMI media to obtain  $1 \times 10^4$  conidia/mL and seeded into each well of 96-well plates. The testing media was RPMI 1640 (Gibco-BRL, Uxbridge, UK) with L-glutamine (without sodium bicarbonate, pH 7.0) adjusted with 0.165 M morpholinepropanesulphonic acid (MOPS).<sup>31</sup> Serial base 2x dilutions of various drugs (50 to 0.006 mg/L) were prepared in RPMI-1640 and added to the wells of microtiter plates in 100- $\mu$ L aliquots. Media alone (200  $\mu$ L) was used as positive control of mycelia growth and 200  $\mu$ L of media alone without conidia was used as negative control. The plates were further incubated for 48 hours at 35 °C and observed under light microscopy for the growth of mycelia. MICs were the lowest drug concentrations that produced complete growth inhibition (100%) at 48 h of incubation.

**Protein Crystallization, Data Collection, Structure Refinement, and Analysis.** For crystallographic experiments, *A. fumigatus* CYP51B was purified in three steps, including anion exchange chromatography

1  
2  
3 on DEAE-Sepharose, affinity chromatography on Ni<sup>2+</sup>-NTA agarose, and cation exchange chromatography  
4 on CM-Sepharose.<sup>9</sup> A 10 μM solution of compound **3** was added to all the buffers at the CM-Sepharose  
5 stage of the purification procedure. The co-crystals were obtained by the hanging drop vapour diffusion  
6 technique and were grown at 16 °C. Equal volumes of complex solution preincubated with 10 mM  
7 cyclohexylpentanoyl-*N*-hydroxyethylglucamide (Anagrade) were mixed with well solution (0.2 M lithium  
8 acetate (pH 7.4) with 19% PEG 3350 (w/v). Crystals appeared after three days and were cryoprotected in  
9 40% glycerol (v/v) and flash-cooled in liquid nitrogen.  
10  
11

12  
13  
14  
15  
16  
17 The data were collected at 100 K using synchrotron radiation on the insertion device of the Life Sciences  
18 Collaborative Access Team at the Advanced Photon Source, Argonne National Laboratory (Argonne, IL),  
19 beamline 21-ID-F at a wavelength of 0.9787 Å and using a Rayonix MX300 CCD detector. The diffraction  
20 images were processed with HKL-2000 in the hexagonal space group P3<sub>1</sub> to maximum resolution of 2.38 Å,  
21 and the structure was solved in Phaser MR (CCP4 Program Suite version 7.0.050) using atomic coordinates  
22 of the voriconazole-bound *A. fumigatus* CYP51 (PDB ID 4UYM). Iterative models of the protein-inhibitor  
23 complexes were built with Coot<sup>32</sup> and refined with Refmac5 in the CCP4 Suite.<sup>33</sup>  
24  
25  
26  
27  
28  
29  
30  
31  
32  
33

### 34 Associated Content

#### 35 Supporting Information:

36  
37  
38 The Supporting Information includes Table S1 (Data collection and refinement statistics) and six  
39 supplementary figures: Figure S1. Structural formulas of systemic antifungal agents, Figure S2.  
40 Apparent ligand binding affinity vs. inhibition of CYP51 activity, Figure S3. Gatekeeping  
41 interactions of LFV in complexes A and B, Figure S4. <sup>1</sup>H NMR spectra, Figure S5. HRMS spectra,  
42 Figure S6. HPLC chromatograms (PDF), and Molecular Formula Strings (CSV).  
43  
44  
45  
46  
47  
48

#### 49 PDB ID Codes:

50  
51 The coordinates and structure factors of *A. fumigatus* CYP51 in complex with compound **3** have  
52 been deposited to PDB under accession code 6CR2. The atomic coordinates and experimental data  
53 will be released upon acceptance of the article for publication.  
54  
55  
56  
57  
58  
59  
60

1  
2  
3 Corresponding Author Information:

4 \*G.I.L. e-mail: galina.i.lepesheva@vanderbilt.edu; phone: 615-343-1373

6  
7 Author Contributions:

8 The manuscript was written through contributions of all authors. All authors have given approval to  
9 the final version of the manuscript.  
10  
11

12  
13 Notes:

14 The authors declare no competing financial interest.  
15  
16

17 Acknowledgment:

18 The work was supported by funding from the National Institutes of Health (GM067871, G.I.L.).  
19  
20 Vanderbilt University is a member institution of the Life Sciences Collaborative Access Team at  
21 Sector 21 of the Advanced Photon Source (Argonne, IL). Use of the Advanced Photon Source at  
22 Argonne National Laboratory was supported by the United States Department of Energy, Office of  
23 Science, Office of Basic Energy Sciences, under Contract DE-AC02-06CH11357. The authors also  
24 would like to thank Prof. Stephen W. Fesik's group for providing access to their Agilent LC-MS and  
25 Biotage Initiator Microwave System.  
26  
27  
28  
29  
30  
31  
32  
33

34 Abbreviations Used:

35 CYP, cytochrome P450; CYP51, sterol 14 $\alpha$ -demethylase; IC<sub>50</sub>, inhibitor concentration that decreases  
36 enzyme turnover rate by 50%; MIC, minimal inhibitory concentration; IFI, invasive fungal infections;  
37  
38 DMF, *N,N*-dimethylformamide; DPPA, diphenyl phosphorazidate; DBU, 1,5-  
39 diazabicyclo[5.4.0]undec-7-ene; THF, tetrahydrofuran; HPLC, high-performance liquid  
40 chromatography; Pd(dppf)Cl<sub>2</sub>, [1,1'-bis(diphenylphosphino)ferrocene]dichloropalladium(II); LC-MS,  
41 Liquid chromatography–mass spectrometry; ESI Electrospray ionization; MS, mass spectrometry;  
42  
43 DMSO, dimethyl sulfoxide; TFA, Trifluoroacetic acid; ELSD, evaporative light scattering detector; rt,  
44 room temperature; equiv., equivalent; h, hours; Hz, Hertz; *J*, coupling constant (in NMR  
45 spectrometry); t<sub>R</sub> retention time (in chromatography); TMS, tetramethylsilane; NMR, nuclear  
46  
47  
48  
49  
50  
51  
52  
53  
54  
55  
56  
57  
58  
59  
60



1  
2  
3 magnetic resonance; MHz, megahertz; DMAP, 4-(N,N-dimethylamino)pyridine; MW, microwave  
4  
5 reactor; EDC/HCl, N-(3-dimethylaminopropyl)-N'-ethylcarbodiimide hydrochloride.  
6  
7  
8  
9  
10  
11  
12  
13  
14  
15  
16  
17  
18  
19  
20  
21  
22  
23  
24  
25  
26  
27  
28  
29  
30  
31  
32  
33  
34  
35  
36  
37  
38  
39  
40  
41  
42  
43  
44  
45  
46  
47  
48  
49  
50  
51  
52  
53  
54  
55  
56  
57  
58  
59  
60

## REFERENCES

- (1) Bongomin, F.; Gago, S.; Oladele, R. O.; Denning, D. W., Global and multi-national prevalence of fungal diseases-estimate precision. *J. Fungi (Basel, Switzerland)* **2017**, *3* (4) pii: E57. doi: 10.3390/jof3040057.
- (2) Pappas, P. G.; Kauffman, C. A.; Andes, D. R.; Clancy, C. J.; Marr, K. A.; Ostrosky-Zeichner, L.; Reboli, A. C.; Schuster, M. G.; Vazquez, J. A.; Walsh, T. J.; Zaoutis, T. E.; Sobel, J. D., Clinical practice guideline for the management of candidiasis: 2016 Update by the infectious diseases society of America. *Clin. Infect. Dis.* **2016**, *62* (4), e1-e50.
- (3) Brown, G. D.; Denning, D. W.; Gow, N. A. R.; Levitz, S. M.; Netea, M. G.; White, T. C., Hidden killers: human fungal infections. *Sci. Trans. Med.* **2012**, *4* (165), 165rv13.
- (4) Denning, D. W.; Hope, W. W., Therapy for fungal diseases: opportunities and priorities. *Trends Microbiol.* **2010**, *18* (5), 195-204.
- (5) Kullberg, B. J.; Arendrup, M. C., Invasive candidiasis. *N.Engl. J. Med.* **2015**, *373* (15), 1445-1456.
- (6) Denning, D. W.; Bromley, M. J., How to bolster the antifungal pipeline. *Science* **2015**, *347* (6229), 1414-1416.
- (7) Lepesheva, G. I.; Friggeri, L.; Waterman, M. R., CYP51 as drug targets for fungi and protozoan parasites: past, present and future. *Parasitology* **2018**, 1-17.
- (8) Maertens, J. A.; Raad, I. I.; Marr, K. A.; Patterson, T. F.; Kontoyannis, D. P.; Cornely, O. A.; Bow, E. J.; Rahav, G.; Neofytos, D.; Aoun, M.; Baddley, J. W.; Giladi, M.; Heinz, W. J.; Herbrecht, R.; Hope, W.; Karthaus, M.; Lee, D.-G.; Lortholary, O.; Morrison, V. A.; Oren, I.; Selleslag, D.; Shoham, S.; Thompson, G. R.; Lee, M.; Maher, R. M.; Schmitt-Hoffmann, A.-H.; Zeiher, B.; Ullmann, A. J., Isavuconazole versus voriconazole for primary treatment of invasive mould disease caused by *Aspergillus* and other filamentous fungi (SECURE): a phase 3, randomised-controlled, non-inferiority trial. *Lancet* **2016**, *387* (10020), 760-769.
- (9) Hargrove, T. Y.; Wawrzak, Z.; Lamb, D. C.; Guengerich, F. P.; Lepesheva, G. I., Structure-Functional Characterization of Cytochrome P450 Sterol 14 $\alpha$ -Demethylase (CYP51B) from *Aspergillus fumigatus* and molecular basis for the development of antifungal drugs. *J. Biol. Chem.* **2015**, *290* (39), 23916-23934.

1  
2  
3 (10) Hargrove, T. Y.; Friggeri, L.; Wawrzak, Z.; Qi, A.; Hoekstra, W. J.; Schotzinger, R. J.; York, J. D.;  
4 Guengerich, F. P.; Lepesheva, G. I., Structural analyses of *Candida albicans* sterol 14 $\alpha$ -demethylase  
5 complexed with azole drugs address the molecular basis of azole-mediated inhibition of fungal sterol  
6 biosynthesis. *J. Biol. Chem.* **2017**, *292* (16), 6728-6743.

10  
11 (11) Hargrove, T. Y.; Garvey, E. P.; Hoekstra, W. J.; Yates, C. M.; Wawrzak, Z.; Rachakonda, G.; Villalta, F.;  
12 Lepesheva, G. I., Crystal structure of the new investigational drug candidate VT-1598 in complex with  
13 *Aspergillus fumigatus* sterol 14 $\alpha$ -demethylase provides insights into its broad-spectrum antifungal  
14 activity. *Antimicrob. Agents Chemother.* **2017**, *61* (7) pii: e00570-17.

19  
20 (12) Lepesheva, G. I.; Park, H. W.; Hargrove, T. Y.; Vanhollebeke, B.; Wawrzak, Z.; Harp, J. M.;  
21 Sundaramoorthy, M.; Nes, W. D.; Pays, E.; Chaudhuri, M.; Villalta, F.; Waterman, M. R., Crystal structures of  
22 *Trypanosoma brucei* sterol 14 $\alpha$ -demethylase and implications for selective treatment of human infections.  
23 *J. Biol. Chem.* **2010**, *285* (3), 1773-1780.

27  
28 (13) Villalta, F.; Dobish, M. C.; Nde, P. N.; Kleshchenko, Y. Y.; Hargrove, T. Y.; Johnson, C. A.; Waterman, M.  
29 R.; Johnston, J. N.; Lepesheva, G. I., VNI cures acute and chronic experimental Chagas disease. *J. Infect. Dis.*  
30 **2013**, *208* (3), 504-511.

33  
34 (14) Friggeri, L.; Hargrove, T. Y.; Rachakonda, G.; Williams, A. D.; Wawrzak, Z.; Di Santo, R.; De Vita, D.;  
35 Waterman, M. R.; Tortorella, S.; Villalta, F.; Lepesheva, G. I., Structural basis for rational design of inhibitors  
36 targeting *Trypanosoma cruzi* sterol 14 $\alpha$ -demethylase: Two regions of the enzyme molecule potentiate its  
37 inhibition. *J. Med. Chem.* **2014**, *57* (15), 6704-6717.

41  
42 (15) Hargrove, T. Y.; Wawrzak, Z.; Alexander, P. W.; Chaplin, J. H.; Keenan, M.; Charman, S. A.; Perez, C. J.;  
43 Waterman, M. R.; Chatelain, E.; Lepesheva, G. I., Complexes of *Trypanosoma cruzi* sterol 14 $\alpha$ -demethylase  
44 (CYP51) with two pyridine-based drug candidates for Chagas disease: Structural basis for pathogen  
45 selectivity. *J. Biol. Chem.* **2013**, *288* (44), 31602-31615.

49  
50 (16) Lepesheva, G. I.; Ott, R. D.; Hargrove, T. Y.; Kleshchenko, Y. Y.; Schuster, I.; Nes, W. D.; Hill, G. C.;  
51 Villalta, F.; Waterman, M. R., Sterol 14 $\alpha$ -demethylase as a potential target for antitrypanosomal therapy:  
52 Enzyme inhibition and parasite cell growth. *Chem. Biol.* **2007**, *14* (11), 1283-1293.

1  
2  
3 (17) Andriani, G.; Amata, E.; Beatty, J.; Clements, Z.; Coffey, B. J.; Courtemanche, G.; Devine, W.; Erath, J.;  
4  
5 Juda, C. E.; Wawrzak, Z.; Wood, J. T.; Lepesheva, G. I.; Rodriguez, A.; Pollastri, M. P., Antitrypanosomal lead  
6  
7 discovery: Identification of a ligand-efficient inhibitor of *Trypanosoma cruzi* CYP51 and parasite growth. *J.*  
8  
9 *Med. Chem.* **2013**, *56* (6), 2556-2567.

10  
11 (18) Lepesheva, G. I.; Hargrove, T. Y.; Rachakonda, G.; Wawrzak, Z.; Pomel, S.; Cojean, S.; Nde, P. N.; Nes,  
12  
13 W. D.; Locuson, C. W.; Calcutt, M. W.; Waterman, M. R.; Daniels, J. S.; Loiseau, P. M.; Villalta, F., VFV as a  
14  
15 new effective CYP51 structure-derived drug candidate for Chagas disease and visceral leishmaniasis. *J.*  
16  
17 *Infect. Dis.* **2015**, *212* (9), 1439-1448.

18  
19 (19) Heeres, J.; Meerpoel, L.; Lewi, P., Conazoles. *Molecules* **2010**, *15* (6), 4129-4188.

20  
21 (20) Van den Bossche, H.; Willemsens, G.; Cools, W.; Cornelissen, F.; Lauwers, W. F.; van Cutsem, J. M., In  
22  
23 vitro and in vivo effects of the antimycotic drug ketoconazole on sterol synthesis. *Antimicrob. Agents*  
24  
25 *Chemother.* **1980**, *17* (6), 922-928.

26  
27 (21) Aoyama, Y.; Yoshida, Y.; Sato, R., Yeast cytochrome P-450 catalyzing lanosterol 14 $\alpha$ -demethylation. II.  
28  
29 Lanosterol metabolism by purified P-450(14)DM and by intact microsomes. *J. Biol. Chem.* **1984**, *259* (3),  
30  
31 1661-1666.

32  
33 (22) Correia, M. A.; Ortiz de Montellano, P. R., Inhibition of Cytochrome P450 Enzymes. In *Cytochrome*  
34  
35 *P450: Structure, Mechanism, and Biochemistry*, 3<sup>rd</sup> ed., Ortiz de Montellano, P. R., Ed., Plenum Publishing  
36  
37 Corp: New York, 2005; pp 246-322.

38  
39 (23) Yoshida, Y.; Aoyama, Y., Interaction of azole antifungal agents with cytochrome P-450<sub>14DM</sub> purified  
40  
41 from *Saccharomyces cerevisiae* microsomes. *Biochem. Pharmacol.* **1987**, *36* (2), 229-235.

42  
43 (24) Lepesheva, G. I.; Waterman, M. R., Structural basis for conservation in the CYP51 family. *Biochim.*  
44  
45 *Biophys. Acta* **2011**, *1814* (1), 88-93.

46  
47 (25) Lepesheva, G. I.; Waterman, M. R., Sterol 14 $\alpha$ -demethylase (CYP51) as a therapeutic target for  
48  
49 human trypanosomiasis and leishmaniasis. *Curr. Top. Med. Chem.* **2011**, *11* (16), 2060-2071.

1  
2  
3 (26) Hargrove, T. Y.; Friggeri, L.; Wawrzak, Z.; Sivakumaran, S.; Yazlovitskaya, E. M.; Hiebert, S. W.;  
4  
5 Guengerich, F. P.; Waterman, M. R.; Lepesheva, G. I., Human sterol 14 $\alpha$ -demethylase as a target for  
6  
7 anticancer chemotherapy: towards structure-aided drug design. *J.Lipid Res.* **2016**, *57* (8), 1552-1563.

8  
9 (27) Yu, X.; Nandekar, P.; Mustafa, G.; Cojocaru, V.; Lepesheva, G. I.; Wade, R. C., Ligand tunnels in *T.*  
10  
11 *brucei* and human CYP51: Insights for parasite-specific drug design. *Biochim. Biophys. Acta* **2016**, *1860* (1,  
12  
13 Part A), 67-78.

14  
15 (28) Friggeri, L.; Scipione, L.; Costi, R.; Kaiser, M.; Moraca, F.; Zamperini, C.; Botta, B.; Di Santo, R.; De Vita,  
16  
17 D.; Brun, R.; Tortorella, S., New promising compounds with in vitro nanomolar activity against *Trypanosoma*  
18  
19 *cruzi*. *ACS Med. Chem. Lett.* **2013**, *4* (6), 538-541.

20  
21 (29) Schenkman, J. B.; Remmer, H.; Estabrook, R. W., Spectral studies of drug interaction with hepatic  
22  
23 microsomal cytochrome. *Mol. Pharmacol.* **1967**, *3* (2), 113-123.

24  
25 (30) Wayne, P. CLSI Reference Method for Broth Dilution Antifungal Ausceptibility Testing of Filamentous  
26  
27 *Fungi*. 3rd edition. CLSI standard M38. Clinical and Laboratory Standards Institute. (2017).

28  
29 (31) Espinel-Ingroff, A.; Turnidge, J.; Alastruey-Izquierdo, A.; Dannaoui, E.; Garcia-Effron, G.; Guinea, J.;  
30  
31 Kidd, S.; Pelaez, T.; Sanguinetti, M.; Meletiadis, J.; Botterel, F.; Bustamante, B.; Chen, Y. C.; Chakrabarti, A.;  
32  
33 Chowdhary, A.; Chryssanthou, E.; Cordoba, S.; Gonzalez, G. M.; Guarro, J.; Johnson, E. M.; Kus, J. V.; Lass-  
34  
35 Florl, C.; Linares-Sicilia, M. J.; Martin-Mazuelos, E.; Negri, C. E.; Pfaller, M. A.; Tortorano, A. M.,  
36  
37 Posaconazole MIC distributions for *Aspergillus fumigatus* Species complex by four methods: Impact of  
38  
39 CYP51A mutations on estimation of epidemiological cutoff values. *Antimicrob. Agents Chemother.* **2018**, *62*  
40  
41 (4). pii: e01916-17. doi: 10.1128/AAC.01916-17.

42  
43 (32) Emsley, P.; Lohkamp, B.; Scott, W. G.; Cowtan, K., Features and development of Coot. *Acta*  
44  
45 *Crystallogr. D Biol. Crystallogr.* **2010**, *66* (4), 486-501.

46  
47 (33) Potterton, E.; Briggs, P.; Turkenburg, M.; Dodson, E., A graphical user interface to the CCP4 program  
48  
49 suite. *Acta crystallogr. D, Biol. Crystallogr.* **2003**, *59* (Pt 7), 1131-1137.

## Table of Contents Graphic

